*Physics – Uspekhi* **45** (8) 793 – 817 (2002) 

*REVIEWS OF TOPICAL PROBLEMS* PACS numbers: **03.30.+p**, 0.7.60.Vg, 42.81.Pa

# Physical problems of fiber gyroscopy based on the Sagnac effect

I A Andronova, G B Malykin

DOI: 10.1070/PU2002v045n08ABEH001073

## Contents



**Abstract. This review is concerned with the physical problems of fiber ring interferometry which underlies the fiber-optic gyroscopy harnessing the Sagnac effect. Locally reciprocal and locally nonreciprocal physical effects are considered, including polarization, transient, magnetic, nonlinear, and relativistic effects. These effects are responsible for the appearance of additional signals, which are similar to the rotation signal, at the output of a fiber-optic gyroscope. The causes of instability of the effects leading to the drift of the output signal are analyzed. The sources of fluctuations which limit the ultimate sensitivity of fiber gyroscopes are considered. We discuss different fields of application of fiber ring interferometers and fiber gyroscopes built around them for practical purposes and to basic research. The prospects for further development of fiber gyroscopy are considered.**

## 1. Introduction

We pursued several goals by bringing readers' notice to this review on fiber gyroscopy. One goal was to commemorate the 50th anniversary of the publication of the work by I L Bershteĭn (22.11.1908 – 16.08.2000), a Professor of the Gor'ky (now Nizhniĭ Novgorod) State University, in which he first proposed and realized a multiturn ring interferometer for measuring the Sagnac effect [1]. The interferometer was made not of glass fiber, but of a radio frequency cable and was intended for measurements in the radio frequency band at a wavelength of 10 m. Despite this fact, this work of Prof. I L Bershteĭn may be considered as laying the groundwork for present-day fiber gyroscopy: the idea of utilizing a multiturn coil as a ring interferometer, which permits improving the sensitivity to rotation due to the Sagnac effect in proportion to the tuned circuit length with little or no changes of interferometer dimensions, was sounded for the first time in this paper. The patent on a multiturn optical glass fiber interferometer was applied for by A Wallace in 1958, eight years after the issue of Bershteĭn's paper. This invention was patented five years later, in 1963 [2]. The idea was first realized in practice in 1976 [3, 4], namely, 18 years after Wallace's patent pending.

The prime objective of our review is to sum up the physical investigations in the realm of fiber ring interferometry, which were undertaken in several research centers during the past 25 years to bring into being the modern fiber gyroscopy and by now are basically complete. At this stage the bulk of the effort goes into the production of gyroscopic devices. However, further improvement of the ultimate sensitivity and stability of fiber gyroscopes, as well as a diversity of technical problems involving minimization of their dimensions and cost, up to now remain a topical problem.

The majority of reviews on fiber gyroscopy known to us [5 – 25] were written during the period when the research had not been completed. To date we can cast a retrospective glance at the physical problems encountered. Furthermore, we can classify from a more general standpoint the physical

**I A Andronova, G B Malykin** Institute of Applied Physics, Russian Academy of Sciences,
ul. Ul'yanova 46, 603950 Nizhniĭ Novgorod, Russian Federation
Tel. (7-8312) 38-43 70, 38-45 67
E-mail: andr@ufp.appl.sci-nnov.ru; malykin@mail.ru

Received 13 July 2001, revised 6 November 2001
*Uspekhi Fizicheskikh Nauk* **172** (8) 849 – 873 (2002)
Translated by E N Ragozin; edited by A Radzig

effects responsible for the appearance of additional optical signals at the output of a fiber-optic gyroscope (FOG), which are identical with the rotation signal, reveal the causes of their possible instability, and elucidate the nature of sensitivity-limiting phenomena.

One further objective of our review is to adequately reflect the contribution of researchers of our country to the advent and development of fiber gyroscopy, because references to the journal publications in Russian are, as a rule, missing from the majority of foreign reviews and original papers.

Also considered in our review is the application of fiber ring interferometers (FRIs) and FOGs built around them to the solution of practical problems and to basic research. We will also discuss the avenues and prospects of the further development of fiber gyroscopy. Moreover, we will touch upon the problems arising in the investigation of the Sagnac effect for waves of unlike nature in different frequency ranges. The technical and technological aspects of FOG development will not be discussed below.

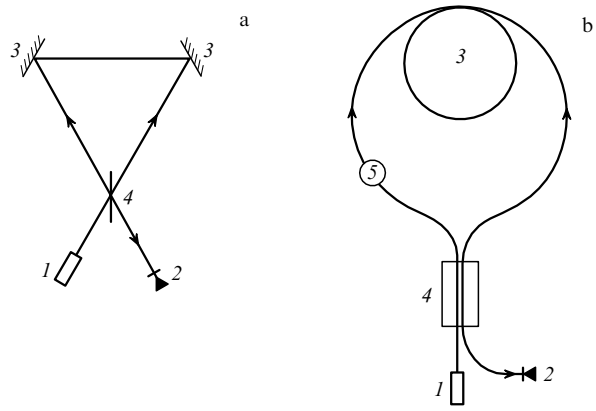


**Figure 1.** Ring Sagnac interferometer: (a) discrete version [(*1*) radiation source, (*2*) photodetector, (*3*) reflectors, (*4*) beam splitter], and (b) all-fiber version [(*1*) radiation source, (*2*) photodetector, (*3*) multiturn fiber circuit, (*4*) fiber beam splitter, (*5*) phase modulator].

## 2. The Sagnac effect

We begin our review with a brief excursion to the history of the Sagnac effect (see Refs [26 – 31]). Consider a closed circuit which rotates about an axis normal to its plane. The heart of the Sagnac effect which underlies the operation of optical gyroscopes is that the difference in phase incursions $\varphi^+ - \varphi^- = \Phi_S$ of two light waves travelling in the closed circuit in opposite directions (Fig. 1a) is proportional to the angular rotational velocity $\Omega$ and the area $S$ of the circuit traced by the counterpropagating waves. The idea that the effect may exist was originally proposed by O Lodge in 1893 [32]; also, he was the first to obtain an expression for the phase difference of the counterpropagating waves

$$\Phi_S = \frac{8\pi S}{\lambda c}\,\Omega\,, \tag{1}$$

where $\lambda$ is the light wavelength, and $c$ is the speed of light.

In the case when the circuit is a circle with the diameter $R$ and perimeter $L = 2\pi R$, the relationship between the phase difference and the rotational velocity can also be represented in the following form

$$\Phi_S = \frac{4\pi RL}{\lambda c}\,\Omega = \frac{8\pi^2 R^2}{\lambda c}\,\Omega = \frac{2L^2}{\lambda c}\,\Omega\,. \tag{2}$$

In 1904, Michelson [33] also obtained expression (1) independently of Lodge. The first experiments were launched by F Harress in 1909 – 1911 employing a prism ring interferometer 40 cm in diameter located on a rotating stage, whose rotational velocity amounted to 600 revolutions per minute [34]. The light source was a mercury arc lamp powered by a current of 20 A. Red and green light filters were placed in turn at the lamp output. The shift of interference fringes in rotating the stage in the opposite directions, which was recorded with a photographic plate, was attributed by Harress not to the rotation, but to the effect of entrainment of light by a rotating prism glass. He believed that without the optical medium the interferometer rotation would not have resulted in the interference fringe shift.

Deliberate experiments on measuring the influence of rotation on the phase difference of counterpropagating waves were first conducted by G Sagnac in 1913 [35, 36], and the effect observed was justly named for its discoverer. In Sagnac's experiment the advantage was taken of a mirror ring interferometer measuring 0.5 m for a base rotational velocity of 50 – 140 rpm. The radiation source was an incandescent lamp, the light at its output being polarized with a Nicol prism. A comparison of the photographs of the interference pattern at the output of the interferometer rotating in the opposite directions allowed a determination of the phase difference arising in the rotation and, hence, a determination of the angular velocity $\Omega$ of the object to which the interferometer was attached. The integral of the phase difference taken over the duration of rotation permitted one to determine the rotation angle of the object. It is pertinent to note that Sagnac was the first to propose exploiting this effect for the purposes of gyroscopy and navigation [37]. The experiment to reveal the rotation of the Earth with the aid of the Sagnac effect was first accomplished by A Michelson, H Gale, and F Pearson in 1925 [38, 39]. They compared the phase difference of the counterpropagating waves in a rectangular interferometer measuring 630 m by 340 m and in an interferometer one side of which coincided with a side of the first interferometer, while the area was close to zero. The light propagated through steel tubes 30 cm in diameter from which the air was evacuated to a pressure of 12 Torr. In these experiments use was made of an arc light source excited by a 25-A current. The phase difference related to the rotation of the Earth was visually measured from the difference in location of the interference fringes taken from two interferometers. The measurement was made 269 times by different people and with replacement of the specular reflectors. Upon averaging, the figure arrived at was 0.236 fringe $\pm 0.002$ fringe, which coincided, to a high degree of accuracy, with the value calculated from the Earth rotation. The project was financially supported primarily by the University of Chicago and cost 17.5 thousand dollars. This experiment actually made a start on optical navigational gyroscopy, i.e. gyroscopy which determines the latitude of a place by measuring the rotational velocity of the Earth. Subsequent optical experiments were aimed at elucidating the influence of the medium on the phase difference in the rotation, which is discussed in considerable detail in the reviews [26 – 28, 30, 31] and the review section of Ref. [40]. The suggestions for measuring the rotational velocity from the shift of resonance frequencies for oppositely directed waves in passive ring resonators were made at a substantially later time [41] (see Fig. 2a).

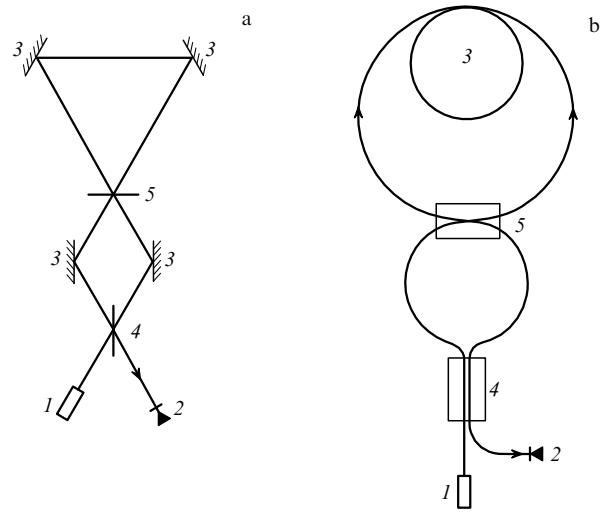


**Figure 2.** Resonance ring Sagnac interferometer: (a) discrete version [(*1*) radiation source, (*2*) photodetector, (*3*) reflectors, (*4*) beam splitter, (*5*) partially transmitting reflector], and (b) all-fiber version [(*1*) radiation source, (*2*) photodetector, (*3*) multiturn fiber circuit, (*4*) fiber beam splitter, (*5*) fiber reflector].

Apart from the optical range, by now the Sagnac effect has been recorded in the radio frequency range [1], the X-ray range [42], and for de Broglie waves of material particles: neutrons [43], electrons [40], and calcium [44], sodium [45], and caesium [46] atoms. Furthermore, the Sagnac effect was considered for the interference of counterpropagating surface acoustic and magnetostatic waves [47, 48], and de Broglie waves of $\pi$-mesons [49]. We note that the sensitivity of measuring the angular rotational velocity in these interferometers should be significantly higher than in FOGs, since the de Broglie wavelengths of atoms and elementary particles are many orders of magnitude shorter than the light wavelength. In particular, even in the first experiments on atomic sodium interferometers [45], the sensitivity was equal to 0.6 deg $h^{-1}$, and to 0.004 deg $h^{-1}$ for atomic caesium interferometers [46].

In the general case, the Sagnac effect should be treated in the context of the general theory of relativity (GTR). However, when the rotation is uniform and it is possible to neglect the space curvature caused by gravitation, the results of Sagnac effect calculations performed in the context of the GTR and in the context of the special theory of relativity (STR) coincide [50, 51]. In the framework of the STR, the Sagnac effect is a consequence of the relativistic law of velocity composition — the linear velocity of interferometer rotation and the phase velocities of counterpropagating waves [48, 52]. The expression for $\Phi_S$ obtained in the framework of the STR is of the form [28, 48, 50–52]

$$\Phi_S = \frac{8\pi S\Omega}{\lambda c(1 - R^2\Omega^2/c^2)^{1/2}} K. \tag{3}$$

In the general case, the coefficient $K$ is defined in relation to the mutual motion of the medium, the reflectors, the light source, and the detector and may contain the effective refractive index of the medium and its dispersion [28, 31, 48, 52]. When the light source, the detector, the medium, and the reflectors are placed on a rotating platform, $K = 1$ and, hence, $\Phi_S$ is independent of the refractive index and material dispersion [48, 52].

We emphasize that there exist a variety of papers in the scientific literature wherein the relationship between $\Phi_S$ and $\Omega$ is derived on the basis of mistaken concepts, including the nonrelativistic law of velocity composition, the Doppler effect for counterpropagating waves incident on the mirrors that move during rotation, etc. The fallacies made by different authors were analyzed in detail in Ref. [52].

Here are the main c o n c l u s i o n s of this section:

— the Sagnac effect is a consequence of the relativistic law of velocity composition, and

— when all elements of the ring interferometer are located on a rotating platform, the phase difference of counterpropagating waves is independent of the refractive index and material dispersion.

## 3. Optical gyroscopy harnessing the Sagnac effect

Optical gyroscopy made its appearance in addition to mechanical gyroscopy which takes advantage of the property of rotating bodies to retain the spatial direction of the rotation axis. This makes it possible to determine the rotation angle of an object relative to the axis of a gyroscope in the gimbal mount. Among the factors that favor the development of optical gyroscopy are the quest to reduce the volume and mass of the instruments, the quest to lower the total cost of navigation systems, and also the effort to shorten their readiness time.

Figure 1a is a schematic of a classical ring interferometer built around discrete elements. It is noteworthy that there exists one more version of optical gyroscopy with the use of a passive ring resonator proposed by A Rosenthal [41] in 1962, which was first implemented around discrete elements in 1978 [53] (Fig. 2a).

Laser gyroscopy became one of the branches of optical gyroscopy based on the Sagnac effect. It takes advantage of the following fact: when two counterpropagating waves are generated in a laser with a ring resonator, their phase difference associated with rotation is transformed to a difference in oscillation frequencies of the counterpropagating waves:

$$\Delta\nu_S = \Phi_S \frac{c}{L},$$

which carries the information about the rotation. The idea of laser gyroscopy was put forward, like that of a passive ring resonator, by A Rosenthal [41] in 1962. The development of laser gyroscopy, which was initiated in 1963 [54], has its own history and scores big successes. Its physical and technical aspects are the concern of reviews [55–59]. To date, several companies are known to have launched the batch production of laser gyroscopes. Among the best-known foreign companies mention should be made of Honeywell, Litton, Sperry, etc., and among the Russian manufacturers we mention M F Stel'makh Scientific-Industrial Association NPO 'Polyus' (Moscow). The sensitivity of modern navigation laser gyroscopes is at the level of 0.01–0.001 deg $h^{-1}$. Laser gyroscopes are used as navigation instruments on submarines, rockets, and airplanes, including American airplanes of the Boeing Co. Furthermore, there are known unique laboratory laser gyroscopes with a higher sensitivity (0.00005 deg $h^{-1}$) [60–63], which are employed for the solution of basic problems, in particular, to measure the degree of nonuniformity of the Earth rotation associated

with the influence of the Moon and other celestial bodies and also with the effect of tectonic mass displacements in the Earth's crust. The monolithic block resonators of these laser gyroscopes, whose perimeter amounts to 3 m and more, are made of a material with a very low thermal expansion coefficient. These lasers are operated in shafts to obviate acoustic vibrations and temperature drops. In our review we deal with passive optical gyroscopy which does not harness lasing.

Using a multiturn coil permits the enhancement of the Sagnac effect in proportion to the fiber length, i.e. to the number of turns in the circuit, with little or no changes in device dimensions. In a multiturn circuit, the expression for the phase difference $\Phi_S$ of counterpropagating waves can be represented in several equivalent forms

$$\Phi_S = \frac{8\pi N s}{\lambda c}\,\Omega = \frac{4\pi R L}{\lambda c}\,\Omega = \frac{8\pi^2 R^2 N}{\lambda c}\,\Omega = \frac{2L^2}{\lambda c N}\,\Omega\,, \qquad (4)$$

where $s = \pi R^2$ is the area of one turn, $N$ is the number of turns, $R$ is the radius of a turn, and $L = 2\pi R N$ is the overall length of the multiturn coil. The device dimensions are determined primarily by the coil diameter ($2R$) and height. The latter in due course depends on the fiber length and the outer diameter of the fiber cladding ($\sim 200$ μm), the number of turns and winding layers and is, as a rule, substantially smaller than the diameter. A comparison of expressions (1), (2), and (4) shows that the sensitivity increases as the square of the total fiber length in a single-turn circuit ($N = 1$), and in proportion to the total length in a multiturn circuit. Therefore, the highest sensitivity for a given fiber length can be obtained only with the use of a single-turn circuit.

It is pertinent to note that not only single-mode, but also multimode low-loss optical fibers had not been fabricated by the moment A Wallace was granted a patent for the invention of a fiber-optic gyroscope [2]. This idea was forgotten for some time, the more so as the year of 1963 saw the realization of the idea of a laser gyroscope. The idea of a fiber gyroscope was put forward for the second time ten years later, in 1968 [64]. By that time the developers of laser gyroscopes had run into several difficulties associated with the necessity of using devices to bring the operating point out of the locking band of counterpropagating waves for low rotational velocities and with a variety of unwanted effects, including nonlinear (diffraction, polarization), magnetic, and some other effects, on the frequency difference of counterpropagating waves. It was not long before considerable progress was made in the fabrication of low-loss single-mode fibers (SMFs), in mastering the technology of welding fibers, and in the development of components of optical sensors (beam splitters, polarizers, phase modulators, etc.). The absence of active elements, low radiation-damage susceptibility, small energy consumption, and low dimensions of fiber gyroscopes engendered the confidence that it would not be long till fiber ring interferometers (FRIs) underlay the development of simple, inexpensive, and compact medium-precision gyroscopes with the prospect of developing the navigation gyroscopes with a precision of better than 0.01 deg $h^{-1}$. However, about ten years passed from the first demonstration of the principle [3], which dates to 1976, to the development of a prototype, and no less than 15 years to the batch production of fiber gyroscopes. This is because both the physical and technical problems arose in the path of designing these devices, requiring the above period of time to be overcome. It is pertinent to note that no less than 15 years were also spent before the concept of a laser gyroscope was embodied in its batch production. But even at the present time it is invalid to say that all the problems of both laser gyroscopy and fiber gyroscopy harnessing the Sagnac effect have been completely solved.

The main c o n c l u s i o n s of this section are as follows. Sagnac-effect optical gyroscopy is realized in three versions:

*active version* — a ring laser, in which rotation brings about a difference in laser frequencies of the counterpropagating waves, and

*passive versions*: a fiber ring interferometer, where rotation results in the phase difference of counterpropagating waves (I-FOG in the English-language literature), and a passive ring fiber (or integral) resonator, where rotation gives rise to an eigenfrequency difference and a phase difference of counterpropagating waves close to the resonance (R-FOG in the English-language literature).

## 4. Fiber gyroscopy employing ring interferometers

### 4.1 Lines of development of fiber gyroscopy

Fiber gyroscopy based on the Sagnac effect took two paths distinguished by employing resonance and nonresonance interference schemes. At the heart of interference nonresonance FOG schemes lies the traditional fiber ring Sagnac interferometer (FRI), in which the measurements are taken of the phase difference of counterpropagating waves bypassing around the circuit once (Fig. 1b). In resonance schemes, advantage is taken of a passive multipass optical ring resonator (Fig. 2b), wherein the measurements are made of the rotation-induced shift of resonance frequencies of the counterpropagating waves or their phase difference in the neighborhood of resonance [23]. We emphasize that the shift of resonance frequencies $\Delta\nu_S$ related to the Sagnac effect does not depend on the length of a multiturn resonance circuit, but depends only on the circuit radius, since $\Delta\nu_S = \Phi_S \cdot c/L$ and $\Phi_S$ is, in accordance with expression (4), proportional to the circuit length and radius. Increasing the circuit length, where it is not associated with losses, leads to a growth of the circuit $Q$ and accordingly to a reduction of the resonator bandwidth ($\Delta\nu_S \sim 1/L$). This may increase precision in the determination of the difference of resonance frequencies or phase difference of the counterpropagating waves in the vicinity of resonance. For several reasons, the resonance FOG has been considerably less studied to date and has not reached the stage of batch production. A consideration of different physical reasons for the lowering of its precision is the subject of a special study and does not come within the province of the present work. Our review is concerned with the investigations of a nonresonance FOG built around an FRI scheme with a single-mode fiber; the former is most widespread and has been brought to the stage of batch production.

In due time an effort was mounted to develop FRIs around inexpensive multimode fiber-optic waveguides [65–67] and also around irregular fibers in which single-mode segments alternate randomly with the few-mode ones [68, 69]. As shown by Andreev et al. [70], even an insignificant departure from the single-mode pattern results in the occurrence of an additional unstable phase difference of the counterpropagating waves at the FRI output. At a later time

this research was terminated. At present, the circuit winding is made only of single-mode fibers — isotropic or anisotropic. In the latter case there is a significant difference in refractive indices for the two orthogonal axes.

The simplest schematic of an FRI is shown in Fig. 1b. The fiber circuit comprises a multiturn coil with the fiber ranging from several hundred meters to several kilometers in length, depending on the purpose of the gyroscope. A beam splitter *4* — an analogue of a beam-splitting plate in discrete optics — may be welded or polished. In a weld-fabricated beam splitter, two fibers are brought close together for a length of $\sim 1$ cm owing to heating and stretching in such a way that the optical field from one fiber penetrates the other one to the requisite degree. Then, the fibers are welded together in an electric arc discharge. The polished beam splitter consists of two quartz plates in which Π-shaped cuts are milled along the surface, with the cut depth increasing towards the plate edges. The fibers are glued into the cuts. Then, the plates are polished to approach the fiber light-guiding core so that the optical field mutually penetrates from one fiber into the other on gluing the plates together, i.e. beam splitting occurs. The signal from the FRI output arrives at a photodetector whose electric current is proportional to the number of incident radiation photons, i.e. the radiation intensity. The photodetector is therefore a quadratic detector of the optical field. When the interference condition is fulfilled, the photocurrent $i$ at the interferometer output is written in the simplest case as

$$i \cong \left[\mathbf{E}^{+}\exp\left\{\mathrm{i}\left(\omega t+\frac{\Phi_{\mathrm{S}}}{2}\right)\right\}+\mathbf{E}^{-}\exp\left\{\mathrm{i}\left(\omega t-\frac{\Phi_{\mathrm{S}}}{2}\right)\right\}\right]^{2}$$
$$=\left|\mathbf{E}^{+}\right|^{2}+\left|\mathbf{E}^{-}\right|^{2}+\left|\mathbf{E}^{+}\right|\left|\mathbf{E}^{-}\right|\cos\Phi_{\mathrm{S}}=2I(1+\cos\Phi_{\mathrm{S}})\,, \tag{5}$$

where $\omega = 2\pi\nu$, and $\nu$ is the optical frequency; $\mathbf{E}^{+}$, $\mathbf{E}^{-}$ are the electric field vectors of the counterpropagating waves at the interferometer output; $I = |\mathbf{E}^{+}|^{2} + |\mathbf{E}^{-}|^{2}$, and $\Phi_{\mathrm{S}}$ is the phase difference of the counterpropagating waves, which is related to the rotational velocity, the fiber length, and the number of turns of the fiber circuit through expressions (4).

The main c o n c l u s i o n s of this section are as follows. An FOG can be made on the basis of an FRI as well as a fiber ring resonator. At the same time, an FRI can underlie not only FOGs, but also the instruments for measuring other physical effects (see Section 8). Therefore, the FOG and FRI concepts do not necessarily coincide.

### 4.2 Methods for maximizing the sensitivity of fiber gyroscopes

The signal recorded at the interferometer output is, according to expression (5), proportional to the cosine of the phase difference. Hence, the scheme in Figs 1a and 1b will exhibit a low sensitivity to rotation and will be insensitive to the sense (sign) of rotation for rotational velocities at which $\Phi_{\mathrm{S}}$ is close to 0 or $n\pi$ (see Fig. 3a). That is why one of the first problems of fiber gyroscopy was the problem of obtaining a constant coefficient of proportionality between the angular rotational velocity and the output signal over a wide range of angular velocities.

One of the most obvious ways of sensitivity maximization, including that for a low rotational velocity, is to shift the operating point to a steep portion of the interference signal dependence on the phase difference of counterpropagating waves (Fig. 3a). Different suggestions were discussed in the scientific literature concerning the shift of the operating point to a steep portion: thanks to an additional nonreciprocal phase, or by mounting the instrument on a rotating or vibrating stage, or with the aid of a nonreciprocal phase element on the basis of the Faraday effect [71] (see Section 5.5). Subsequently, to measure the phase difference of counterpropagating waves for low angular velocities the advantage was taken of the splitting of counterpropagating-wave frequencies [72, 73] employing discrete [74] or fiber [75] acousto-optical modulators and the measurement of the interference signal phase at the difference frequency employing synchronous detection. The suggestions were also made that the FRI operating point can be shifted by using the nonlinear optical Kerr effect (see Section 5.6), when the counterpropagating-wave intensities are different [76, 77], or through the use of a special $3 \times 3$ splitter at the FRI input to produce an initial phase difference of counterpropagating waves [78–80]; the wave front mismatch of counterpropagating waves [81]; the polarization nonreciprocity (see Section 5.3) by virtue of turning the axes of linear anisotropy of the SMF circuit at the FRI input in the presence of a circularly polarized radiation component [82], and also with the aid of losses in the input beam splitter [83]. However, all the above-enumerated techniques of reaching the maximum sensitivity have not found practical use.

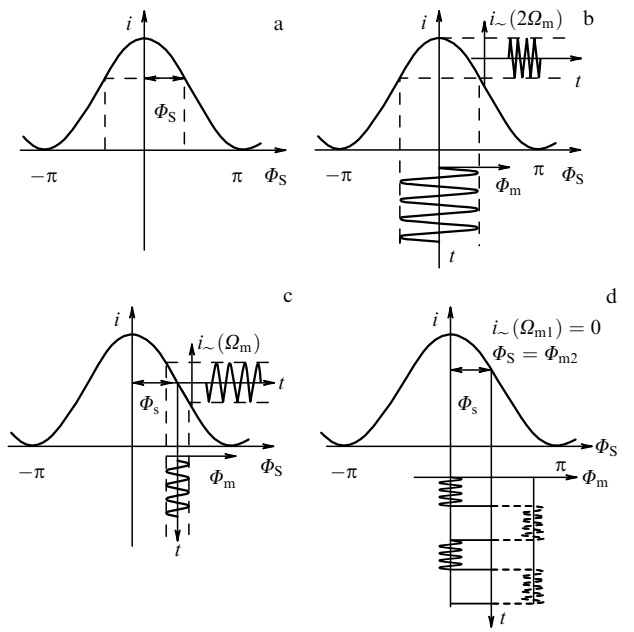


**Figure 3.** (a) Photocurrent $i$ (output intensity) of a fiber ring interferometer (FRI) as a function of the phase difference $\Phi_{\mathrm{S}}$ of counterpropagating waves. (b) Scheme for obtaining the rotation-generated signal in the modulation measuring technique ($\Phi_{\mathrm{m}}$ and $\Omega_{\mathrm{m}}$ are the amplitude and frequency of modulation, respectively, and $t$ is the time); for $\Phi_{\mathrm{S}} = 0$, the signal retains only even harmonics of the modulation frequency. (c) The same as in Fig. 3b, but for $\Phi_{\mathrm{S}} \neq 0$; in the output signal there appear odd harmonics of the modulation frequency $\Omega_{\mathrm{m}}$. (d) Modulation (compensation) technique for measuring the Sagnac phase with the use of double phase modulation at a high frequency $\Omega_{\mathrm{m1}}$ with an amplitude $\Phi_{\mathrm{m1}}$ and at a low frequency $\Omega_{\mathrm{m2}}$ with an amplitude $\Phi_{\mathrm{m2}}$; measurements are made in $\Phi_{\mathrm{m2}}$ for $\Phi_{\mathrm{m2}} = \Phi_{\mathrm{S}}$, which is the case when the output signal at the frequency $\Omega_{\mathrm{m1}}$ vanishes [$i_{\sim}(\Omega_{\mathrm{m1}}) = 0$].

The most fruitful method among a wide range of proposed methods is that of asymmetric phase modulation effected at one of the ends of the fiber coil [84, 85]. Notice that

this idea was first put forward in D McLaughlin's patent for a ring interferometer based on discrete elements [86] as early as 1965. The phase modulation in the fiber interferometer is accomplished with the aid of either a piezoceramic modulator, or an integrated-optical modulator. In the piezoceramic modulator, a small fraction of the circuit fiber is wound around the piezoceramics, which is most often cylindrical in shape. The fiber length and thereby the transmitted radiation phase change under the influence of electric voltage applied to the ceramics. In the integrated-optical modulator, advantage is taken of the refractive index dependence for the planar-optical-waveguide crystal material ($LiNbO_3$) on the applied a.c. voltage. For an asymmetric position of the modulator in the fiber circuit, one wave passes through the modulator at entry into the circuit, and the other at exit, i.e. in a time $\tau = nL/c$ (where $n$ is the refractive index of the fiber light-guiding core) taken to travel the entire length $L$ of the fiber circuit. The result is that the modulation phase of one wave differs from the modulation phase of the counterpropagating wave by a value of $\Omega_m\tau$, where $\Omega_m$ is the circular modulation frequency. In this case, the interference signal is written in the form

$$i = I\Big[1 + \cos\big(\Phi_S + \Phi_m \cos\Omega_m t - \Phi_m \cos(\Omega_m t + \Omega_m\tau)\big)\Big] = I\left[1 + \cos\left\{\Phi_S + 2\Phi_m \sin\left(\frac{\Omega_m\tau}{2}\right)\sin\left(\Omega_m t + \frac{\Omega_m\tau}{2}\right)\right\}\right]. \quad (6)$$

We employ the Bessel functions to expand the expression for the photocurrent (6) in terms of the harmonics of the modulation frequency to obtain the following result for the photocurrent

$$i = 2I\left[1 + J_0\left(2\Phi_m \sin\frac{\Omega_m\tau}{2}\right)\right]\cos\Phi_S + 4IJ_1\left(2\Phi_m \sin\frac{\Omega_m\tau}{2}\right)\sin\Phi_S \cos\left[\Omega_m\left(t - \frac{\tau}{2}\right)\right] + 4IJ_2\left(2\Phi_m \sin\frac{\Omega_m\tau}{2}\right)\cos\Phi_S \cos\left[2\Omega_m\left(t - \frac{\tau}{2}\right)\right] + \ldots, \quad (7)$$

where $J_0$, $J_1$, and $J_2$ are the corresponding-order Bessel functions of the first kind. The photocurrent $i$ is the sum of harmonics whose amplitudes depend on the intensity $I$ of counterpropagating waves and the values of the Bessel functions in which the argument is defined by the quantity $2\Phi_m \sin(\Omega_m\tau/2)$.

Therefore, the photocurrent $i$ depends on the amplitude $\Phi_m$ and frequency $\Omega_m$ of phase modulation and on the time $\tau$ defining the delay of modulation of one wave relative to the counterrunning one. In the absence of rotation one has $\Phi_S = 0$, and the output photocurrent contains only even harmonics of the modulation frequency (Fig. 3b). In the presence of rotation or any other nonreciprocal phase difference, there appear odd harmonics of the modulation frequency as well (Fig. 3c). To measure the rotational velocity, as a rule, advantage is taken of the first harmonic of the modulation frequency, whose amplitude depends, according to expression (7), on the value of the first-order Bessel function and the value of $\sin\Phi_S$ and, hence, changes sign on changing the sense of rotation. This dependence is shown in Fig. 4 for different rotational velocities. One can see from the figure that the amplitude of the first harmonic of the modulation frequency has a peak corresponding to the maximum of the first-order Bessel function. As a rule, this value of the modulation amplitude is selected as the working one. At present, the technique of asymmetric phase modulation [85, 87, 88] is employed in the majority of fiber gyroscopes. For measurements over a wide velocity range, compensation techniques are particularly attractive, which automatically produce a signal compensating for the rotation signal in their operation. In this case, the rotational velocity is measured from the magnitude of the compensating signal. To produce the compensating signal, in some cases additional low-frequency phase modulation is taken into consideration [88]. The principle of the double phase modulation technique is presented in Fig. 3d. The low-frequency modulation, typically in the form of a meander, is performed along with the sinusoidal, high-frequency one. The receiver rejects one low-frequency half-period [87, 88]. The rotational velocity is determined from the value of a low-frequency amplitude at which the first high-frequency harmonic vanishes.

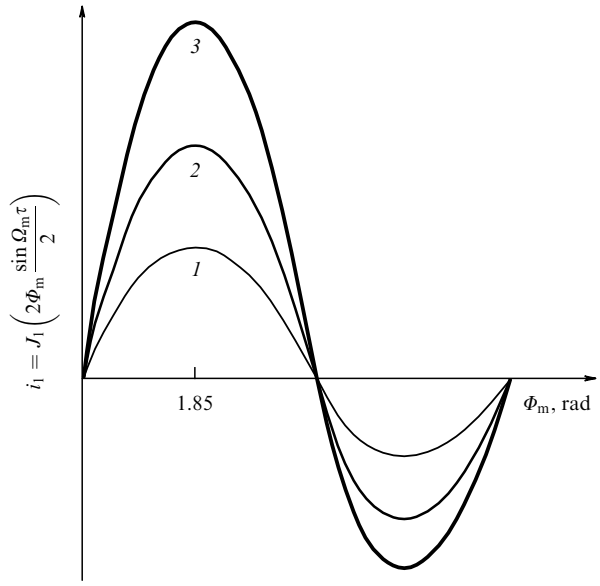


**Figure 4.** Amplitude of the first harmonic of the interference signal $i_1$ as a function of the amplitude $\Phi_m$ of phase modulation for three values of the Sagnac phase: $\Phi_{S1}$ (curve *1*); $\Phi_{S2}$ (curve *2*), and $\Phi_{S3}$ (curve *3*) ($\Phi_{S1} < \Phi_{S2} < \Phi_{S3} < \pi/2$).

Among the techniques that allow an expansion of the velocity measurement range is the technique which involves measuring the entire set of harmonics of the modulation frequency in the photocurrent. This permits the phase shift to be measured even though the first-harmonic amplitude may vanish. Furthermore, there exist well-known techniques for measuring the rotational signal whereat use is made of electro- or acousto-optical devices to produce a frequency difference of the counterrunning waves with subsequent measurement of the phase of the difference-frequency signal. These issues will be additionally considered in Section 6.

## 5. Sources of additional nonreciprocity in fiber gyroscopes

Experimental FRI research revealed the appearance of additional signals at the interferometer output, which are identical with the rotation signal but not related to rotation.

Signals of this kind were not observed in classical Sagnac experiments. In the course of development of fiber gyroscopy, a considerable effort was mounted to determine the underlying physical causes and the means to eliminate these signals. These studies showed that the sources of additional signals may be divided into several groups. Effects related to the scattering and reflection of light in the fiber circuit fall into the first group. The second group incorporates the effect of polarization nonreciprocity (PN) related to the asymmetric arrangement (noncommutativity) of anisotropic elements relative to the middle of the fiber circuit or their orientation or the anisotropic fiber properties. Among the effects of the third group are those associated with locally reciprocal transient changes of the fiber parameters in their excitation asymmetrically relative to the middle of the fiber circuit. The fourth group encompasses properly nonreciprocal effects, such as the Faraday effect, the Fresnel – Fizeau effect, and some others. The effects caused by the nonlinear optical Kerr effect fall into the fifth group. And finally, the effects of special (STR) and general (GTR) relativity theories make up the sixth group.

Let us consider in greater detail the causes for the occurrence of additional signals, whose instability may have a profound influence on the characteristics of fiber gyroscopes.

### 5.1 Additional signals as a consequence of the coherence of radiation sources

In the first FOGs [3, 4, 85], the function of a radiation source was fulfilled by a He-Ne laser with a wavelength of 0.63 μm, which is a source of coherent monochromatic radiation. That is why among the first effects discovered was the effect related to the coherence of the laser radiation sources employed, which did not show up in classical Sagnac experiments. Back reflections [89, 90] and backward scattering, including Rayleigh scattering [91 – 94], in the optical path of a fiber gyroscope produce an arbitrarily phased additional signal unrelated to rotation. Under the coherent addition to the useful signal, this gives rise to an additional phase difference $\Phi_1$ of counterpropagating waves at the FRI output. Furthermore, the reflections and the scattering bring about a retroaction of the laser, and the laser radiation turns out to be modulated in the frequency of the phase modulator. This distorts the magnitude of the output signal measured at the modulation frequency. Different ways to suppress the back action on the laser were discussed in the scientific literature, including the placement of an optical isolator at the laser output and the use of additional phase modulation at the laser output to destroy the phase coupling between the radiation emanating from the laser and that going from the interferometer back to the laser [72, 73, 95].

However, the radical measure which eliminated the effect of back reflections and backscattering on both the radiation source and the signal being measured was the change-over from monochromatic sources — lasers — to semiconductor broadband superluminescence diodes (SLDs) — new-generation radiation sources with a high spectral intensity and a short coherence length (10 – 20 μm) [96]. In this case, the signals scattered from different elements and different segments of the fiber circuit do not interfere with the signals that carry the information on rotation and do not change their phase owing to the short coherence length. That is why since the early 1980s SLDs came into use in lieu of lasers in fiber gyroscopes [96]. We note that recently a start was made on the employment of superfluorescence fiber sources on active fibers (SFSs), which are characterized by a large spectral width and significant radiation intensity [97 – 99]. The demand for broadband radiation sources for fiber gyroscopy led to the development of their production. This in turn marked a new stage in the evolution of low-coherence interferometry which had been in the background since the advent of lasers. Low-coherence interferometry with new radiation sources has gained acceptance in those fields of optics that require separation of the signals originating from different layers of an object. This opportunity emerges in the sequential observation of the interference pattern from different layers through varying the length of the interferometer reference arm. The resolving power of this interferogram is determined by the source coherence length and is equal to about 10 μm for present-day SLDs. Along with fiber gyroscopy, optical coherence tomography came to be one of the most promising fields of low-coherence fiber interferometry [100]. The harnessing of tomography for medical purposes makes it possible to obtain layer-by-layer interference patterns for the radiation scattered by a biological tissue. This permits one to determine the internal tissue structure up to a depth of 2 mm with a resolution of $\sim 10$ μm without disturbing the biological tissue under investigation. This holds much significance for noninvasive diagnostics of tissue pathologies and for the statement of diagnosis.

The main c o n c l u s i o n of this section is as follows: the use of nonmonochromatic radiation practically obviates the problem arising from the influence of reflected and scattered radiation on the phase of the FRI output signal.

### 5.2 Techniques for calculating additional signals

The employment of SLDs obviated only a part of the problems brought about by the appearance of additional signals at the FRI output that are not related to rotation. There arose a demand for analyzing and calculating FRI schemes to derive the complete picture of possible nonreciprocal effects in the interference signal. The Jones matrix method [101 – 110] proved to be the most popular and convenient way of calculating the FRI schemes containing single-mode anisotropic fiber and anisotropic elements. This method is commonly employed to determine the variations of a polarization state and the phase of light in its transmission through optical systems containing a sequence of anisotropic optical elements. In the context of the Jones matrix method, the light polarization state at a given point in space is described by a complex vector, while its transformation by an anisotropic element (or a combination of anisotropic elements) is described by a linear operator. In a Cartesian coordinate system, this operator is represented with a 2-by-2 Jones matrix. To every anisotropic element there corresponds a matrix of its own. To derive the resultant matrix for the sequence of FRI anisotropic elements, recourse is made to a standard procedure [111] to transform the matrices of all the elements to a common coordinate system with their subsequent multiplication in the order corresponding to the order of their transmission by each of the two counterrunning waves. Multiplying the matrices gives the resultant matrices $\widehat{M}^+$ and $\widehat{M}^-$ of the FRI for the oppositely directed waves. Employing the Jones matrix method enables one to collect in a general form information on the occurrence of additional signals at the FRI output. The Jones matrices of an FRI are

written as

$$\widehat{M}^{+} = \begin{vmatrix} M_{11}^{+} & M_{12}^{+} \\ M_{21}^{+} & M_{22}^{+} \end{vmatrix}, \quad \widehat{M}^{-} = \begin{vmatrix} M_{11}^{-} & M_{12}^{-} \\ M_{21}^{-} & M_{22}^{-} \end{vmatrix}. \tag{8}$$

The expressions for the FRI matrix elements depend on the fiber parameters and the elements of a specific scheme. These expressions in concrete cases can be found in Refs [82, 112–120].

In the absence of nonreciprocal effects (rotation, magnetic field, etc.), a fiber ring interferometer must satisfy the conditions of the traditional reciprocity theorem [121, 122], which are written in the following form for the elements of the Jones matrices [123]:

$$M_{11}^{+} = M_{11}^{-}, \quad M_{22}^{+} = M_{22}^{-}, \quad M_{12}^{+} = M_{21}^{-}, \quad M_{21}^{+} = M_{12}^{-}. \tag{9}$$

We prescribe in complex form the column vector of the electric field of the light wave at the FRI input as

$$\mathbf{A} = \begin{vmatrix} A_x \\ A_y \exp(\mathrm{i}\psi) \end{vmatrix}$$

(where $\psi$ is the phase difference of the orthogonal components of the electric field) to obtain the following matrix equation for the field vectors $\mathbf{E}^{+}$ and $\mathbf{E}^{-}$ of counterpropagating waves at the FRI output:

$$\mathbf{E}^{+} = \widehat{M}^{+}\mathbf{A}, \qquad \mathbf{E}^{-} = \widehat{M}^{-}\mathbf{A}. \tag{10}$$

By solving these equations for both propagation directions with the aid of the elements of the Jones matrix we obtain the vector field components of the counterpropagating waves at the FRI output:

$$\begin{aligned} E_x^{+} &= M_{11}^{+}A_x + M_{12}^{+}A_y \exp(\mathrm{i}\,\psi), \\ E_y^{+} &= M_{21}^{+}A_x + M_{22}^{+}A_y \exp(\mathrm{i}\,\psi), \\ E_x^{-} &= M_{11}^{-}A_x + M_{12}^{-}A_y \exp(\mathrm{i}\,\psi), \\ E_y^{-} &= M_{12}^{-}A_x + M_{22}^{-}A_y \exp(\mathrm{i}\,\psi). \end{aligned} \tag{11}$$

The interference signal at the FRI output is of the form $U = E_x^{+}E_x^{-*} + E_y^{+}E_y^{-*}$. Notice that the quantity $U$ is the trace of the coherence matrix of the counterpropagating waves in the FRI [107, 110]. The signal recorded by the photodetector at the output is determined by the value of $\mathrm{Re}\,U$, and the nonreciprocal phase difference $\Phi$ of counterpropagating waves is given by the relationship

$$\Phi = \arctan\left[\frac{\mathrm{Im}\,U}{\mathrm{Re}\,U}\right]. \tag{12}$$

The expressions for $U$, $\mathrm{Re}\,U$, $\mathrm{Im}\,U$, and $\Phi$ in the general form, given in terms of FRI matrix elements, appear in Refs [119, 120, 124]. An analysis of expression (12) for the phase difference $\Phi$ at the FRI output shows that additional terms unrelated to rotation may be present in the general case, apart from the terms determined by properly nonreciprocal effects (the Sagnac, Faraday, and Fresnel – Fizeau effects), for which the FRI matrices do not meet the reciprocity conditions (9). The instability of these additional terms during the gyroscope operation can also influence the accuracy of rotation velocity measurements. Strictly speaking, calculations by the Jones matrix method can only be done for monochromatic radiation. Nevertheless, with the use of the coherence matrix this method may be applied to nonmonochromatic radiation as well [82, 114–118]. When applying the numerical simulation technique, calculations of the output signal for broadband radiation sources are performed by the Jones matrix method for a finite number of spectral components. The interval between the components is determined by the path length and the birefringence of the FRI SMF circuit, and their number by the radiation source bandwidth. The resultant signal is obtained by summation over all wavelengths [125–128].

Here is the main c o n c l u s i o n of this section: the Jones matrix method represents an adequate method for calculating the signal at the FRI output for monochromatic and broadband radiation sources, which finds applications both in analytical calculations and in numerical simulation of the output signal.

We now turn to a more detailed consideration of the sources of additional signals at the FRI output.

### 5.3 Polarization nonreciprocity: causes of its occurrence and ways of elimination

The effect of polarization nonreciprocity, which was observed even in the first experimental FRI investigations in 1976 [3], turned out to be the least evident effect unrelated to rotation in FRIs. This effect had not been previously recorded in ring interferometers utilizing discrete optical elements. It came as a surprise to researchers, for it emerged in FRIs even when their characteristics satisfied the traditional classical reciprocity theorem [121–123]. It was not long before this effect was interpreted independently by G Schiffner et al. [129], R Ulrich and M Johnson [130], and V N Logozinskiĭ [131] (see also Ref. [132]). As was revealed in the course of investigations, the emergence of this effect is conditioned by the difference of polarizations of counterpropagating waves at the FRI output, which arises despite the fact that their polarizations at the FRI input are similar, because the oppositely directed waves are excited from a common channel. The difference in polarizations at the output is related to the fact that the sequence of passages through the anisotropic elements of the circuit is different for oppositely directed waves. This implies that the commutativity conditions relative to the middle of the fiber circuit are not fulfilled for the elements [119, 120]. This signifies the inequality of the off-diagonal elements of the FRI Jones matrix ($M_{12} \neq M_{21}$) and the occurrence of additional phase nonreciprocity ($\Phi_2$). Such a phenomenon has come to be known as *polarization nonreciprocity* or, more precisely, as the *polarization phase nonreciprocity of counterpropagating waves*.

By now the concept of the 'FRI polarization nonreciprocity' has become firmly established in the terminology of papers on fiber gyroscopy. It is noteworthy that the polarization nonreciprocity effects are in a sense 'virtual' or 'hidden', because revealing them requires the presence of an additional phase difference. This phase difference can be obtained due to a noncoincidence of the fronts in the interference of counterpropagating waves at the output, or due to traditional nonreciprocity effects like the Sagnac, Faraday, and Fresnel – Fizeau effects, or under additional counterpropagating-wave phase modulation asymmetric relative to the middle of the circuit, which is employed in the majority of fiber gyroscope schemes to obtain the information on rotation.

An analysis showed [119, 120] that the FRI interference signal (Re $U$) in the absence of these prerequisites does not carry information about the nonreciprocal phase related to the difference in polarizations of the counterpropagating waves at the output, because the variation of phase is compensated for by the change in amplitude of the interference signal. The researchers who were first to discover the PN effect [3, 4, 133] were fortunate in the sense that the experiments at the initial stage of an FRI development were conducted on semidiscrete schemes, with the additional phase occurring due to the front difference of the interfering waves.

The first PN investigators proposed two different ways of eliminating phase nonreciprocity. The first is based on using two identical linear polarizers with similar orientations of their transmission axes, placed at the ends of the fiber circuit [129, 131, 132]. The second made use of two similarly oriented identical linear polarizers placed after the radiation source and in front of the photodetector [130]. In 1980, Ulrich [85] came up with a third way — the so-called 'minimal scheme' of an FRI, which has the advantage, over the previous two, that it comprises only one polarizer located between two beam splitters in the circuit (Fig. 5). When the radiation is transmitted through the polarizer in the forward and backward directions, its transmission axis is automatically oriented in a similar way, and therefore the 'minimal scheme' of an FRI dispenses with the need for a polarizer alignment. Yet another advantage of this scheme is the measurement of the signal from an additional beam splitter located at the FRI input, making it possible to eliminate the influence of the phase characteristics of the beam splitters on the phase difference of counterpropagating waves. We note that the interference signal at the circuit output carries information about the phase difference between reflection and transmission in the beam splitter located at the circuit input, because one wave experiences two reflections and the counterpropagating wave passes through the beam splitter twice. The use of the 'minimal scheme' of an FRI has gained the widest acceptance in fiber gyroscopy.

In early papers (see, for instance, Ref. [85]), the polarizer in the 'minimal scheme' was assumed to reduce the polarization-nonreciprocity-induced phase shift at the FRI output in proportion to the square of the polarizer coefficient of extinction in the electric field amplitude $\varepsilon$, because the counterpropagating waves pass through the polarizer twice. However, as was later shown by E Kintner [134], the additional phase difference at the output contains terms depending on $\varepsilon^2$ as well as on $\varepsilon$. The interference terms on the order of $\varepsilon$ arise from the products of the electric field vector components for the input wave whose polarization coincides with the polarizer transmission axis at the input and is perpendicular to it at the output.

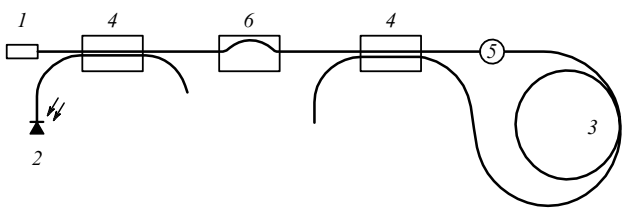


**Figure 5.** 'Minimal scheme' of an FRI: (*1*) radiation source, (*2*) photodetector, (*3*) fiber circuit, (*4*) beam splitters, (*5*) modulator, and (*6*) polarizer.

One of the causes of polarization nonreciprocity, in particular, is associated with the rotation of SMF anisotropy axes with respect to each other at the fiber coil ends (the noncommutativity of anisotropy at the circuit ends) or with a noncoincidence of anisotropy axes of the nonideal beam splitter and the SMF axes at the circuit input. The noncoincidence of the SMF axes at the circuit ends may take place due to their dissimilar fixation or welding together with the ends of an anisotropic beam splitter.

We note that the appearance of an additional phase difference was also attributed in several papers [135–137] to the polarization plane rotation due to the Rytov effect [138–141]. This effect, which is related to the topological features of wave propagation through a mechanically unstressed isotropic fiber wound in a nonplane (helical) manner around a coil, depends on the winding pitch and is a manifestation of the geometrical phase in optics, quite often referred to as the *Berry phase* [142–149]. The Rytov effect by itself is reciprocal, which has been borne out by experiments [137]. That is why the winding pitch influence on the phase difference of counterpropagating waves in an FRI can hardly be attributed to the Rytov effect and the explanations given in the scientific literature [135–137] are likely to be wrong, the more so as this phenomenon has not been found experimentally [150].

As a simple example we consider an FRI (see Fig. 5) designed according to the 'minimal scheme' with one polarizer and a superluminescence radiation source [85]. The fiber circuit of length $L$ is made of a fiber with a regular linear birefringence. The anisotropy axes at the two circuit ends are turned through the angles $\alpha_1$ and $\alpha_2$ with reference to the axes of the laboratory coordinate system. In accordance with Refs [113–115, 119, 120], the expressions for the matrix elements governing this scheme are written as

$$M_{11} = -\left[\cos\Delta\beta_L \frac{L}{2}\cos(\alpha_1+\alpha_2) + \mathrm{i}\,\sin\Delta\beta_L \frac{L}{2}\cos(\alpha_1-\alpha_2)\right],$$
$$M_{22} = -(M_{11})^*,$$
$$M_{12} = -\varepsilon\left[\cos\Delta\beta_L \frac{L}{2}\sin(\alpha_1+\alpha_2) + \mathrm{i}\sin\Delta\beta_L \frac{L}{2}\sin(\alpha_1-\alpha_2)\right],$$
$$M_{12} = (M_{21})^*, \qquad (13)$$

where $\Delta\beta_L = 2\pi/(\lambda\Delta n_L)$ is the linear birefringence; $\Delta n_L = n_x - n_y$ is the difference of the refractive indices in the slow and fast SMF axes; $\lambda$ is the wavelength, and $\varepsilon$ is the in-field polarizer extinction coefficient.

Substituting expressions (13) in formulas (11) we obtain the expressions for counterpropagating wave fields at the output. The result of interfering and the phase difference essentially depend on the degree of coherence of the counterpropagating waves that have travelled along the fast and slow axes of the anisotropic fiber circuit (the two-channel property). For an FRI with a superluminescence radiation source, the waves that have travelled along the fast and slow axes become incoherent and do not interfere, i.e. the two-channel property is absent. In this case, the expression for the nonreciprocal phase $\Phi_2^0$ is written as [114, 115]

$$\Phi_2^0 = \arctan\left[\frac{\mathrm{Im}\,U}{\mathrm{Re}\,U}\right] = \arctan\frac{\varepsilon A_y\,\sin\psi\,\sin 2(\alpha_1-\alpha_2)}{A_x\left[\cos^2(\alpha_1-\alpha_2)+\cos^2(\alpha_1+\alpha_2)\right]}, \qquad (14)$$

where $A_x$, $A_y$, and $\psi$ are the amplitudes and the phase difference of orthogonal radiation components at the FRI input, while $\alpha_1$ and $\alpha_2$ are the angles defining the orientation of SMF anisotropy axes at the circuit input and output with respect to one of the axes of the preferred reference system. From formula (14) it follows that the nonreciprocal phase becomes zero in three cases. In the first case, the anisotropy axes of the fiber ends are not turned ($\alpha_1 = \alpha_2$) and, therefore, $M_{12} = M_{21}$, and the FRI is polarization-reciprocal. In the second case, the interferometer is polarization-nonreciprocal, but there is no phase shift ($\psi = 0$) between the $x$ and $y$ components of the electric field at the interferometer input. In the third case, the electric field component orthogonal to the polarizer transmission axis is absent ($A_y = 0$) at the FRI input. We note that the polarization of radiation at the FRI input does not contain a circular component in the two last-mentioned cases. Therefore, the absence of an additional signal at the output does not necessarily testify to polarization reciprocity.

The authors of Ref. [151] came up with an experimental technique employing a rotating polarizer in front of the photodetector, which allows a statement that the polarization nonreciprocity does or does not occur, this being so at any magnitude of the additional signal at the FRI output. The suppression of polarization nonreciprocity effects with the aid of a polarizer harnessing the dichroism which arises when anisotropic fiber is steeply wound around a coil [152 – 154] was considered in Ref. [155]. Furthermore, there exist polished polarizers with a specially deposited layer [156] which are built around an SMF with a core displaced from the fiber axial line (the so-called *D* fiber) [157], polarizers on the basis of a mechanically stressed SMF [158], fiber polarizers utilizing sodium pentaborate crystals [159], liquid crystals [160], and crystals grown into the fiber cladding [161 – 163]. We note that the effective value of the extinction coefficient of a polarizer in an FRI is limited by an inconsistency between the lateral structure of SMF polarization eigenmodes and the corresponding polarization modes of the polarizer [164 – 166]. The idea of reducing the FRI zero shift by way of incorporating two or more polarizers into the scheme, which was considered in Refs [167, 168], has not found practical use.

It is worth noting that polarization nonreciprocity can be observed even in an FRI from a single-polarization SMF (i.e. an SMF with a large dichroism wherein the second polarization mode experiences very strong losses in comparison with the dominant one and can hardly propagate), when the azimuths of linear anisotropy axes at the circuit ends do not coincide and there exists a circular radiation component at the FRI input ($\psi \neq 0$, $A_y \neq 0$), i.e. when the two-channel property does not emerge [119]. A clear physical explanation for the cause of polarization nonreciprocity in this case is as follows: when the azimuths of SMF anisotropy axes immediately at the input ends of the FRI circuit do not coincide, the counterpropagating waves can acquire an initial phase difference in consequence of a nonsimultaneous excitation of counterpropagating linearly polarized eigenmodes by the circular component of an electric field of the input wave rotating with a light frequency. In Ref. [169], a wrong opinion was stated that PN cannot occur in an FRI with a circuit made of a single-polarization SMF.

The torsional twist owing to mechanical stress, which is produced when a fiber is wound around a coil [170 – 174], may give rise to induced circular birefringence and as a consequence to the ellipticity of the SMF polarization eigenmodes. In this case, the FRI PN also arises when the axes of eigen polarization ellipses at different circuit inputs are turned with respect to each other. However, the nonsimultaneous excitation of elliptically polarized modes at different circuit ends may take place both with a circular and linear polarization of radiation at the FRI input [118, 175]. In the case when the polarization eigenmodes of the SMF circuit of the FRI are circularly polarized, under no state of radiation polarization at the FRI input can PN take place [118, 175]. This is so because the modes have no preferred azimuth and the excitation of circularly polarized modes at both FRI circuit inputs occurs simultaneously under arbitrary state of polarization at the FRI input.

Therefore, the PN phenomenon can in some cases be considered as a high-frequency nonstationarity (nonsimultaneity) in the excitation of counterpropagating waves at different ends of an FRI circuit. The necessary condition for the occurrence of PN in the FRI is a noncoincidence of the azimuths of polarization eigenmodes at both ends of the circuit and a noncoincidence of the polarization state of the exciting electric field at the circuit input with either of them [118, 175, 176].

It is noteworthy that another mechanism of polarization nonreciprocity may exist when use is made of the laser sources. The counterpropagating waves that have travelled along the fast and slow axes of the anisotropic circuit fiber remain coherent or partially coherent, and the noncoincidence of the azimuths of the SMF anisotropy axes at the circuit ends gives rise to the conditions for radiation interference in orthogonal channels. Additional terms related to the interference of coherent components of orthogonal modes, i.e. to the two-channel property, can appear in the signal at the FRI output. The phase of this signal depends on the circuit length $L$ and the magnitude of birefringence, and it can therefore vary under mechanical action on the fiber and temperature variations throughout the length of the circuit fiber. This effect is not reflected in expression (14) derived for a the low-coherence radiation source. However, the presence of the two-channel property alone does not result in the occurrence of PN.

In a number of papers, the placement of a depolarizer in lieu of a polarizer or along with the polarizer was considered with the aim to suppress the PN effects [96, 116, 117, 126, 127, 177 – 188]. A depolarizer is an optical element at whose output the radiation becomes practically depolarized. The degree of residual polarization defines the depolarizer quality. For broadband radiation, advantage is taken of a depolarizer — 'disperser', wherein depolarization is effected by producing uncorrelated radiation of equal intensity in two orthogonal linear anisotropy axes. In the simplest case, the function of a depolarizer can be fulfilled by a linear phase plate or a segment of anisotropic fiber [181] longer than the depolarization length $L_D$, for which the radiation that has been transmitted along the orthogonal anisotropy axes becomes incoherent. The depolarization length is defined by the relation

$$L_D = \frac{\lambda^2}{\Delta\lambda\,\Delta n}\,,$$

where $\lambda$ is the wavelength, $\Delta\lambda$ is the spectral width of the radiation source, and $\Delta n$ is the difference of refractive indices in the slow and fast axes of a phase plate or a fiber segment.

The design of a Lyot depolarizer [189] is more complex; it consists of two phase plates of different length with a linear birefringence whose axes are turned by 45° with respect to each other [190]. The fiber version of the Lyot depolarizer [23, 24, 177, 191–194] involves two anisotropic fiber segments $L_1$ and $L_2$ with a 1:2 length ratio, which are connected in such a way that the segment linear-anisotropy axes are turned through 45°, and $L_1 > L_D$. One other condition should be satisfied when using a depolarizer in an FRI:

$$L_1 \Delta n_d > L \Delta n \,,$$

where $L$ is the fiber length in the circuit, and $\Delta n_d$, $\Delta n$ are the differences of fiber refractive indices of the depolarizer and the circuit.

Figure 6 serves to illustrate the depolarizer operation as a 'dispersion' of pulses (whose length corresponds to the length $l_c$ of a coherent wave train of a broadband radiation source) along orthogonal anisotropy axes ($\Delta l_1$ and $\Delta l_2$). The 'dispersion' has the effect that the pulses (wave trains) in the orthogonal axes become equal in intensity and incoherent at the output of the second segment, because they do not overlap within their length, i.e. within the coherence length. When depolarizers are employed in an FRI scheme, their quantity, location [96, 116, 117, 126, 127, 177, 178], and quality determine the degree of suppression of polarization nonreciprocity effects. The quality is defined by the degree of residual polarization of radiation at the depolarizer output, which in turn is determined by the coupling between orthogonal polarization modes resulting from the inhomogeneities of the depolarizer fiber [174, 177, 194–198]. A version of a continuous fiber depolarizer was proposed in Ref. [199], wherein the turn of segment axes through 45° is effected with the aid of a fiber polarization Lefevre controller [200]. In the case when the depolarizer is located at the circuit input and the radiation is transmitted through it twice, as shown in Refs [117, 126, 127] the polarization may be restored in the second transmission. To avoid it, advantage should be taken of a depolarizer in which the lengths of the two segments satisfy the relationship $2L_1 - L_2 > L_1$, which is fulfilled, in particular, for a length ratio $L_1 : L_2 = 1 : 3$.

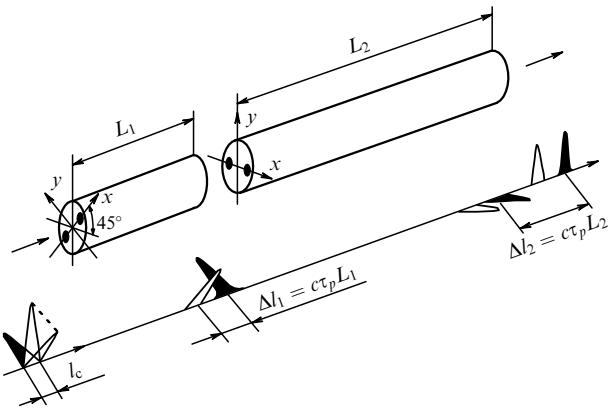


**Figure 6.** Illustrating the operation of a fiber Lyot depolarizer [24]: ($L_1$, $L_2$) lengths of depolarizer segments; ($l_c$) radiation coherence length; ($\tau_p$) difference between the group velocities of light in the orthogonal polarizations of an SMF linear birefringence; ($\Delta l_1$, $\Delta l_2$) optical path differences for the orthogonal polarizations of radiation in the first and second segments.

We note that, along with the above depolarizer types, descriptions of some other types can be found in the scientific literature — both for nonmonochromatic [201–204] and monochromatic radiation. In depolarizers of the latter type, the depolarization of radiation is effected through the action of piezocontrollers [205–208] on the fiber parameters, and also with the aid of a stochastic switch for the radiation polarization state [209].

In the foregoing we neglected the coupling between polarization eigenmodes in the SMF circuit of an FRI. There is good reason to set off and group together the PN effects arising from random mode coupling. It is common practice to characterize the coupling strength by the $h$ parameter [174, 195, 196, 210–213] which defines the relative fraction of the power transferred from one SMF polarization eigenmode to the orthogonal mode over a fiber length of one meter. The causes of random coupling between optical fiber eigenwaves can be divided into natural, arising from the Rayleigh scattering in the light-guiding core [91–94], and technical causes, stemming from the fiber production technology. Real optical fibers are dominated by the technical causes. These include, in particular, random twists of fiber anisotropy axes that emerge during fiber pulling from a work stock, due to the fluctuations of transverse deformations which do not coincide with anisotropy axes, and emerge during protective coating, the fluctuations of the core diameter, etc. As a consequence there occurs a coupling between unperturbed orthogonal linearly polarized fiber eigenmodes, whose dependence along the fiber length can be represented as a random function

$$C(z) = \sqrt{\varepsilon_{xy}(z)} \,,$$

where $\varepsilon_{xy}(z)$ is an off-diagonal element of dielectric susceptibility tensor of the fiber material. Let us introduce the parameter $h$ which is the power spectral density $\Gamma(\Delta\beta_L)$ of the function of spatial distribution of the random coupling between orthogonal modes over the fiber circuit length $C(z)$ at the spatial frequency of polarization beats $\Delta\beta_L = 2\pi/L_b$ ($L_b = \lambda/\Delta n_L$ is the length of polarization beats in an SMF). The quantity $\Gamma(\Delta\beta_L) = h$ is defined in terms of the correlation function $K(u)$ of the random coupling between orthogonal modes $C(z)$. If it is assumed in accordance with Refs [174, 214–217] that the random-coupling correlation coefficient is of the form

$$K(u) = \frac{\langle C(z)\, C(z+u)\rangle}{\langle C^2(z)\rangle} = \exp\left(-\frac{u}{\langle l\rangle}\right), \tag{15}$$

then for the spectral density we obtain

$$\langle \Gamma(\Delta\beta_L)\rangle = h = 2\langle C^2(z)\rangle \int_0^\infty K(u)\, \cos(\Delta\beta_L)\, u\, \mathrm{d}u = \frac{2\langle C^2(z)\rangle\langle l\rangle}{1 + \Delta\beta_L^2 \langle l\rangle^2} \,. \tag{16}$$

In a number of papers [126, 127, 174], the principal mode-coupling mechanism is associated with random fiber twists occurring at those stages of its pulling from the work stock when the fiber has not yet solidified completely, which is in reasonable agreement with available experimental data [218, 219]. According to this model, random twists are responsible for the occurrence of induced circular birefringence, which is randomly distributed in magnitude, sign, and spatial period,

and accordingly of weak ellipticity of fiber eigenmodes, the ellipticity magnitude and sign varying randomly throughout the fiber length. In this case, the coupling coefficient of orthogonal modes is given by

$$C(z) = (1-g)\,\theta(z)\,,$$

where $\theta(z)$ is the dependence of random twist of linear birefringence axes on the fiber length, and $g$ is the photoelasticity coefficient of the SMF material. In accordance with the model posed in Ref. [174], the quantity $\theta$ (rad m$^{-1}$) is uniformly distributed over the interval $[-\theta_{\max}, \theta_{\max}]$ and

$$\langle C^2(z)\rangle = \frac{\left[(1-g)\,\theta_{\max}\right]^2}{3}\,.$$

The length of random segments with a constant torsion obeys the exponential distribution (15). The magnitude of mathematical expectation $\langle l\rangle$, equal to the nonuniformity correlation length, depends on the technology and is equal, as a rule, to $\sim 2.5$ cm [174]. This is significantly shorter than the fiber depolarization length $L_D$ in the case of commonly employed nonmonochromatic radiation sources. In this case, one finds

$$\langle \Gamma(\Delta\beta_L)\rangle = h = \frac{2\left[(1-g)\,\theta_{\max}\right]^2\langle l\rangle}{3\left(1+\Delta\beta_L^2\langle l\rangle^2\right)}\,. \qquad (17)$$

We note that the regular torsion of an SMF with a linear birefringence and a random twist of birefringence axes results in a reduction of the $h$ parameter [220, 221].

There are grounds to believe that the contribution to the coupling between polarization modes from core diameter fluctuations considered in Ref. [222], random fiber stresses, and other factors responsible for the occurrence of random mode coupling is significantly smaller than the contribution from random twists.

We now turn to the consideration of the effect of random coupling between polarization eigenmodes of the fiber, which makes up the FRI circuit winding, on the polarization nonreciprocity of the FRI.

The mode coupling can be interpreted as the existence of a sequence of chaotically located elements in the fiber with somewhat different anisotropy (torsion) parameters. In the passage from one element to another this may result in the radiation transfer from one anisotropy axis to the orthogonal one on the neighboring element, i.e. to the coupling between orthogonal modes. The chaotic location of the elements leads to their noncommutativity with respect to the middle of the circuit, to the inequality between the off-diagonal elements of the Jones matrix of the FRI, and to the occurrence of PN.

We consider here the case

$$hL \ll 1\,, \quad \sqrt{hL_D} \ll 1\,, \quad L_D \gg \langle l\rangle\,,$$

which is typical of an FRI with a circuit from a strongly anisotropic SMF and a superluminescence radiation source having a circuit of length $L \leqslant 1$ km from an SMF with a large linear anisotropy ($\Delta n \sim 10^{-3}-10^{-4}$). In this case, the existence of coupling has the effect that at the input FRI ends within the depolarization length $L_D$ in each of the polarization modes there appear additional coherent components transferred from the orthogonal mode, whose magnitude and phase depend on the magnitude of the $h$ parameter and the length $L_D$. The radiation transferred to the orthogonal mode at the input is responsible for the occurrence of an additional interference signal $\Phi_2'$ at the output. In the presence of a polarizer with an extinction coefficient $\varepsilon$, this signal is equal to an order of magnitude to $\Phi_2' \cong 0.5\varepsilon\sqrt{hL_D}$ [114, 115]. Apart from the effect considered above, multiple coupling-induced radiation transfers from one orthogonal mode to the other throughout the circuit length $L$ in the segments of length $L_D$ mutually symmetric relative to the circuit middle prove to be coherent and produce an additional coherent signal at the output of the FRI scheme [114]:

$$\Phi_2'' \cong 0.5\varepsilon^2 hL_D\sqrt{\frac{L}{L_D}}$$

(the quantity $L/L_D$ is numerically equal to the number of depolarization lengths contained in the circuit length). Note that $\Phi_2' \gg \Phi_2''$.

In the case where the conditions

$$hL \ll 1\,, \quad \sqrt{hL_D} \ll 1\,, \quad L_D \ll \langle l\rangle$$

are fulfilled, which is possible when the radiation source band is broad enough, the reverse situation may occur: $\Phi_2' \ll \Phi_2''$ [223]. To date, the broadest band is offered by a pulsed source employing an air – quartz type light guide ($\Delta\lambda = 1200$ nm) [224].

The temporal variability of the random coupling between polarization modes in counterpropagating waves, arising from heating or mechanical perturbations of the fiber, may result in changes of the magnitude and sign of $\Phi_2'$ and $\Phi_2''$ and, accordingly, in an interference signal phase drift at the FRI output.

A lowering of the $h$ parameter, including that due to regular SMF twisting [220, 221], reduces the degree of polarization of nonmonochromatic radiation as the radiation is transmitted through the SMF [225] and, as a consequence, reduces the temperature drift of the FRI zero. It was shown in Refs [226 – 229] that the asymptotic degree of polarization of low-coherence radiation propagating through a fiber with a random polarization-mode coupling tends to zero as the fiber length approaches infinity. This allows an assumption that the temperature drift of the FRI zero should lower with a significant increase in circuit length.

In the general case, when the conditions $hL \ll 1$, $\sqrt{hL_D} \ll 1$ are not fulfilled, an analytic expression for $\Phi_2'$ and $\Phi_2''$ is impossible to obtain, and the interference signal at the FRI output, caused by polarization-mode coupling, and its drift are calculated by numerical simulations of SMF random nonuniformities [125]. The above-considered effects arising from polarization-mode coupling may be responsible for quite a significant drift of the zero when the FRI circuit makes use of an inexpensive weakly anisotropic fiber, which is characterized by a high $h$-parameter value [125, 197, 230 – 232].

The ways of suppressing the PN in the presence of random mode coupling (the quantities $\Phi_2'$ and $\Phi_2''$), like in the case of turn of the SMF anisotropy axes at the circuit inputs ($\Phi_2^0$), consist in the use of a polarizer or a depolarizer in the FRI scheme.

Papers [233, 234] were concerned with the feasibility of averaging the PN-induced drift of the FRI zero by applying the modulation of the radiation polarization state at the FRI circuit input [234] or in its middle [233]. By now, a series of papers have been published in the scientific literature which

are devoted to the calculation of the PN effects for specific FRI schemes in the presence of polarization-mode coupling, taking advantage of the Jones matrix method and numerical simulations [82, 112–120, 125–127, 150, 181–184, 235–239]. In Refs [175, 176], the geometrical technique of calculating PN with the use of the Poincare sphere [105–107] was considered, i.e. in the Stokes parameter space, and an analogy was drawn between PN and topological effects, such as the Berry phase [142–149] in quantum mechanics or the Rytov phase [138–141] in optics. On the Poincare sphere of unit radius, the $\Phi_2^0$ quantity for the counterpropagating waves of each polarization mode is numerically equal to the area of the spherical triangle made by three points corresponding to the radiation polarization state of a given mode at both circuit outputs and to the radiation polarization state at the FRI input. The Poincare sphere technique applies to simple cases of PN calculations, when the characteristics of a beam splitter and the polarization-mode coupling can be neglected ($\Phi_2' = \Phi_2'' = 0$).

In conclusion we formulate the main results of this section:

(1) We have considered the effects of PN, which are one of the causes of the appearance of additional phase difference at the FRI output. These effects were shown to be related to the difference in polarizations of counterpropagating waves at the output, which in turn is related to the noncommutativity of anisotropic elements and their orientations with respect to the middle of the FRI circuit. Three cases of PN occurrence were considered. In the first two cases we considered a circuit made of uniform anisotropic fiber without polarization-mode coupling, whereas in the third case account was taken of the random coupling between polarization eigenmodes of the FRI circuit.

In the first case, PN arises due to noncoincidence of SMF anisotropy axes at the fiber circuit inputs (the noncommutativity of anisotropy at the inputs) as a consequence of high-frequency nonstationarity — the nonsimultaneous excitation of the input radiation from polarization eigenmode field at two circuit ends. This effect is independent of coherence radiation properties because it emerges at the input, is not related to the excitation of the second orthogonal mode, and is therefore present even in a single-polarization fiber. This effect does not occur when employing an SMF with circularly polarized eigenmodes.

In the second case, PN occurs when three conditions are fulfilled: the two-channel property, i.e. the propagation of counterpropagating wave radiation along two orthogonal modes (channels) in the FRI circuit; coherence or partial coherence of radiation in the orthogonal modes upon transmission through the circuit, and the fulfillment of the prerequisite for their interference due to a noncoincidence of anisotropy axes at the fiber circuit input (output). In this case, the interference signal at the output may carry additional information on the phase difference (polarization) related to fiber birefringence, no matter what the polarization of radiation at the input.

In the third case, PN is caused by the random coupling between orthogonal eigenmodes in the FRI circuit fiber. Because of the coupling, in each orthogonal mode there appears a coherent component of the other mode with a random phase. An additional signal emerges in the interference in coherent components of the orthogonal modes due to the noncommutativity of coupling relative to the middle of the circuit. The magnitude of the signal in the second and third cases may vary under mechanical action on the circuit SMF and under changes of its temperature.

(2) To suppress the PN effects in FRI schemes, in all cases the incorporation of a polarizer or a depolarizer is in common practice.

(3) To calculate the PN effects in simple cases, recourse can be made to the Poincare sphere technique or the Jones matrix method, with account taken of the coherence of the fields which interfere at the output. In more complex cases, including that of a broadband radiation source in the presence of orthogonal-mode coupling, it is possible to resort to numerical computer simulations involving the Jones matrix method for a finite number of spectral radiation components and subsequent integration over the spectrum.

### 5.4 Additional signals under local changes of gyroscope fiber circuit parameters arising from variable acoustical, mechanical, and thermal actions

The third group of additional rotation-unrelated signals ($\Phi_3$) at the FRI output is produced by thermal, mechanical, or acoustical actions on fiber parameters that are locally reciprocal but are excited asymmetrically with respect to the middle of the fiber circuit. These effects are responsible for changes in amplitude, polarization, and phase of one wave, which are delayed in time relative to the counterpropagating wave [240, 241]. These transient actions disturb the FRI-circuit reciprocity conditions. The influence of phase modulation in the circuit on the output signal is given by relationship (7). It follows from the latter that the perturbation with a frequency $\Omega_{\rm inf}$ produces an output signal at a frequency $2\Omega_{\rm inf}$, whose amplitude is defined by the second-order Bessel function $J_2$ of the first kind of an argument $2\Delta\Phi_{\rm inf}\sin\Omega_{\rm inf}\tau/2$, where $\Delta\Phi_{\rm inf}$ is the amplitude of the phase action, and $\tau$ is the time difference of the actions on counterpropagating waves. For $\Delta\Phi_{\rm inf}\sin\Omega_{\rm inf}\tau/2 \ll 1$, the interference signal is proportional to the square of the argument of the Bessel function $J_2$, i.e. $\sim(\Delta\Phi_{\rm inf})^2$. High-frequency perturbations result in higher-amplitude signal perturbations in comparison with low-frequency perturbations of the same intensity. It can be shown with the use of expression (7) that transient effects for counterpropagating waves prove to be out of phase and compensate each other when the condition $\Omega_{\rm inf}\tau = \pi$ is fulfilled [242]. When the rotation signal is recorded at the modulation frequency $\Omega_{\rm m}$, external asymmetric actions at a frequency $\Omega_{\rm inf}$ result in the modulation of the output signal at frequencies $\Omega_{\rm m} \pm \Omega_{\rm inf}$ and an additional, parasitic signal thereby produces actions at frequencies which fall within the reception band $\Delta\Omega$ [243], i.e. $\Omega_{\rm inf} \leqslant \Delta\Omega$.

A separate group of nonreciprocal transient effects is made up of effects related to the operation of the phase modulator itself. It is always located asymmetrically with respect to the middle of the fiber circuit and gives rise to an additional nonreciprocal signal at the second harmonic of the modulation frequency $2\Omega_{\rm m}$ in the absence of the Sagnac effect and (or) other nonreciprocal effects. This signal is usually filtered out owing to the selective reception of the rotation signal at the first harmonic of the modulation frequency.

Along with the phase modulation, the modulation of radiation amplitude and polarization may occur during the modulator operation [242, 244–248]. The polarization modulation of radiation occurs when the phase modulation depths in two orthogonal axes are different. Both the amplitude modulation and the modulation of polarization

produce effects at the first harmonic of the modulation frequency, whose phases are, as a rule, shifted by $\pi/2$ relative to the phase of the rotation signal. In the phase detection they may be removed due to the proper phase selection of the reference signal. In the case when not only the amplitudes, but also the phases of modulation in orthogonal modes are different, the occurrence of a component cophased with the useful signal is a possibility. The effects related to the nonideal operation of a phase modulator were also investigated in Ref. [249]. A technique of the compensation for polarization modulation with the use of a Faraday element reversing the polarization of radiation [250–252] was proposed in Refs [253, 254]. The employment of integrated optical modulators will supposedly permit elimination of the polarization modulation [255–257].

It was shown in Refs [258–260] that the presence of even harmonics, primarily of the second harmonic in the voltage feeding the phase modulator, is responsible for the appearance of an additional signal at the first harmonic, which may be either in phase or in antiphase with the useful signal.

The main c o n c l u s i o n of this section is that only phase, polarization, and amplitude perturbations of counterpropagating waves, which are asymmetric relative to the middle of the fiber circuit and occur at frequencies within the reception bandwidth, can have effect on the phase difference of the counterpropagating waves at the FRI output.

### 5.5 Nonreciprocal effects related to the Faraday effect in an external magnetic field

We consider the influence of an external constant magnetic field as one of the causes for the occurrence of a group-four additional signal ($\Phi_4$) at the FRI output. The effects related to the imposition of magnetic field were considered in Refs [23, 261–267]. The existence of these effects and their instability in the course of operation impair the precision characteristics of fiber gyroscopes and generate the need for magnetic screening. An additional phase incursion in an elementary fiber segment, related to the Faraday effect in a magnetic field, is written as

$$\mathrm{d}\varphi_H = \alpha V \mathbf{H}\,\mathrm{d}\mathbf{z}\,,$$

where $\alpha$ is a coefficient which depends on the polarization state of the propagating radiation and is equal to zero for a linear polarization, and to $\pm 1$ for a circular polarization; $\mathrm{d}\mathbf{z}$ is a vector collinear with the direction of wave propagation; $\mathbf{H}$ is the magnetic field vector whose typical value for terrestrial field is $5\times 10^{-5}$ T, and $V$ is the Verdet constant which is inversely proportional to the square of the wavelength $\lambda$ and equal to 2 rad m$^{-1}$ T$^{-1}$ for $\lambda = 0.85$ μm in quartz. When an SMF is isotropic or exhibits circular birefringence, one has $\alpha = \pm 1$. The existence of linear birefringence of an SMF reduces the magnitude of $\alpha$. The resultant birefringence of an SMF in a magnetic field is determined by its anisotropy and is given by the relationship

$$\Delta\beta_{\pm} = \frac{2\pi(n_+ - n_-)}{\lambda} = \sqrt{\Delta\beta_L^2 + (\Delta\beta_H \pm \Delta\beta_C)^2}\,,$$

where the signs $\pm$ refer to oppositely directed waves; $\Delta\beta_L = 2\pi\Delta n_L/\lambda$ is the reciprocal linear birefringence; $\Delta\beta_C = 2\pi\Delta n_C/\lambda$ is the reciprocal circular birefringence related, according to Refs [170–172, 174], to fiber torsion per unit length $\theta(z)$ by the relationship $\Delta\beta_C(z) = (1-g)\,\theta(z)$, and $\Delta\beta_H = 2\pi\Delta n_H/L = 2VH$ is the nonreciprocal circular birefringence caused by a magnetic field. For quartz fibers, one finds $g = 0.06-0.08$.

The Jones matrix method is conveniently used to calculate magnetic effects for FRI specific fiber parameters and a given magnetic field configuration. The form of the FRI matrix depends on the specific fiber parameters and magnetic field configuration. Let the magnetic field be constant along the SMF ($\mathbf{H}\,\mathrm{d}\mathbf{z} = \mathrm{const}$), which is the case when the coil with wound fiber resides in a toroidal solenoid or envelops a current-guiding conductor and the magnetic lines of force are concentric circles. In this case, the elements of the Jones matrix for an FRI circuit made of an SMF with linear and circular birefringence are of the form

$$\begin{aligned}
M_{11}^{+} &= \cos\Delta\beta_+ L + \mathrm{i}\frac{\Delta\beta_L}{\Delta\beta_+}\sin\Delta\beta_+ L\,,\\
M_{11}^{-} &= \cos\Delta\beta_- L + \mathrm{i}\frac{\Delta\beta_L}{\Delta\beta_-}\sin\Delta\beta_- L\,,\\
M_{22}^{+} &= \cos\Delta\beta_+ L - \mathrm{i}\frac{\Delta\beta_L}{\Delta\beta_+}\sin\Delta\beta_+ L\,,\\
M_{22}^{-} &= \cos\Delta\beta_- L - \mathrm{i}\left(\frac{\Delta\beta_L}{\Delta\beta_-}\right)\sin\Delta\beta_- L\,,\\
M_{12}^{+} &= \frac{(\Delta\beta_H + \Delta\beta_C)\,\sin\Delta\beta_+ L}{\Delta\beta_+}\,,\\
M_{12}^{-} &= \frac{(\Delta\beta_H - \Delta\beta_C)\,\sin\Delta\beta_- L}{\Delta\beta_-}\,,\\
M_{21}^{+} &= -\frac{(\Delta\beta_H + \Delta\beta_C)\,\sin\Delta\beta_+ L}{\Delta\beta_+}\,,\\
M_{21}^{-} &= -\frac{(\Delta\beta_H - \Delta\beta_C)\,\sin\Delta\beta_- L}{\Delta\beta_-}\,.
\end{aligned} \tag{18}$$

For $H \neq 0$, these expressions do not satisfy the reciprocity conditions (9). By substituting expressions (18) into Eqns (11) it is possible to obtain expressions for the orthogonal field components of counterpropagating waves at the output and the phase difference between them. An analysis of the expression for the phase difference of counterpropagating waves in a magnetic field in this case shows that three qualitatively different situations can take place, depending on the type of birefringence of the SMF circuit eigenmodes.

(1) The FRI circuit is made of an isotropic SMF or an SMF with an intrinsic circular birefringence. In this case, the nonreciprocal phase difference is proportional to the polarizer extinction coefficient $\varepsilon$ in the FRI scheme (see Fig. 5) and emerges only when a circular field component is present at the FRI input.

(2) The FRI circuit is made of an SMF with an intrinsic linear birefringence. In this case, the nonreciprocal phase difference is also proportional to the polarizer extinction coefficient $\varepsilon$ and emerges when either a circular component, or a linear one whose direction makes an angle of 45° with the SMF anisotropy axes, or both simultaneously are present at the FRI input.

(3) The FRI circuit is made of an SMF with an intrinsic elliptical birefringence. In this case, there arises a nonreciprocal phase difference related neither to the circular field component, nor to the linear one at an angle of 45°, which

does not depend on the presence of a polarizer in the FRI scheme. For $\Delta\beta_L \gg \Delta\beta_C$, $\Delta\beta_H$, the quantity $\Delta\beta_+ - \Delta\beta_- \approx \Delta\beta_H \Delta\beta_C/\Delta\beta_L$, and the expression for the resultant, polarizer-independent phase difference $\Delta\varphi_H$ at the output of the ring interferometer is written as

$$\Phi_4 = \frac{\oint \Delta\beta_H(z)\,\Delta\beta_C(z)\,\mathrm{d}z}{\Delta\beta_L} = \frac{2V}{\Delta\beta_L}\oint \Delta\beta_C(z)\,\mathbf{H}(z)\,\mathrm{d}\mathbf{z}\,. \quad (19)$$

In a series of papers and reviews (see, for instance, monograph [23]), only the component independent of the polarizer extinction coefficient was regarded as the FRI magnetic responsivity. We emphasize that the above-mentioned situation takes place only when the magnetic field component along the turns of the fiber circuit is nonzero. This may be the case, in particular, when an FRI is employed as a sensor of magnetic field or electric current (see Section 8).

We now consider another wider-spread case when an FRI is embedded in an external magnetic field with a constant direction, which is the case, for instance, under exposure to the terrestrial magnetic field. The projection of magnetic field $\mathbf{H}$ onto an element of length $\mathrm{d}\mathbf{z}$ varies as $\cos(2\pi z/R)$ along a turn, where $R$ is the turn radius, and hence $\oint \mathbf{H}\,\mathrm{d}\mathbf{z} = 0$ at each turn. In this case, the FRI matrix proves to be reciprocal for constant fiber parameters. However, if the fiber parameters are not constant along the circuit length, an additional phase difference may arise in a constant magnetic field. For $\Delta\beta_L \gg \Delta\beta_C$, $\Delta\beta_H$, this phase difference may be calculated using the relationship

$$\Phi_4 = \frac{2VH}{\Delta\beta_L}\oint \Delta\beta_C(z)\,\cos\left(\frac{z}{R} - \varphi\right)\mathrm{d}z\,, \quad (20)$$

where $R$ is the turn radius; $\Delta\beta_L = 2\pi\Delta n_L/\lambda$ is the linear birefringence; $\Delta\beta_C(z) = (1-g)\,\theta(z)$ is the circular birefringence in relation to the $z$-coordinate, and $\varphi$ is the angle between the direction of magnetic field and the straight line passing through the beginning and center of a turn. Integration is performed along the length $L_W$ of a closed turn of the FRI circuit. It is evident from expression (20) that magnetic effects are absent when the torsion is constant along the circuit turn [$\Delta\beta_C(z) = \mathrm{const}$]. The phase difference will be a maximum when the birefringence changes its sign according to the cosine law ($\Delta\beta_C \cong \cos z/R$), i.e. is determined by those components of the torsion spatial spectrum (circular birefringence) $\Gamma_{xy}(2\pi/L_W)$ whose period corresponds to the turn length of the fiber circuit of radius $R$ and $L_W = 2\pi R$. The possible variations of the phase difference at the FRI output due to the changes in the direction of a magnetic field $\Phi_4$ can, according to the results of paper [263], be written in the form

$$\Phi_4 \cong \frac{2HV}{\Delta\beta_L}\sqrt{\hbar L}\,, \quad (21)$$

where $L$ is the circuit length, and $\hbar = \Gamma(2\pi/L_W)$ is the spectral density of the spatial component of circular birefringence, whose spatial period corresponds to the turn length $L_W = 2\pi R$. Like in the determination of the standard parameter $h = \Gamma(2\pi/L_\mathrm{b})$ (where $L_\mathrm{b}$ is the length of polarization beats in an SMF), for the quantity $\hbar$ we will proceed from the model of random twists of SMF axes [174], considered in Section 5.3, and will take advantage of expression (15) for the random-twist correlation function $K(u)$ to eventually obtain

$$\Gamma\left(\frac{2\pi}{L_W}\right) = \hbar = 2\int_0^\infty K(u)\,\cos\left(\frac{2\pi}{L_W}\,u\right)\mathrm{d}u = \frac{2\left[(1-g)\,\theta_\mathrm{max}\right]^2\langle l\rangle}{3\left[1+\langle l\rangle^2/R^2\right]}\,. \quad (22)$$

When the orthogonal-mode coupling parameter $h$ is determined by random twists of fiber axes, for the $h/\hbar$ ratio from expressions (16) and (22) we have

$$\frac{h}{\hbar} = \frac{[1+\langle l\rangle^2/R^2]}{[1+4\pi^2\langle l\rangle^2/L_\mathrm{b}^2]}\,, \quad (23)$$

and for $2\pi R = L_\mathrm{b}$ the magnitude of $\hbar$ is equal to $h$. Putting $\langle l\rangle = 2.5$ cm, $R = 5$ cm, $\theta_\mathrm{max} = 1.92$ rad m, $g = 0.08$, we obtain a value of $\hbar = 4\times10^{-2}$ m$^{-1}$. Substituting the resultant value in formula (21) for an FRI with a circuit length $L = 500$ m and a birefringence $\Delta\beta_L = 2.2\times10^3$, for magnetic effects in the terrestrial field ($H = 5\times10^{-5}$ T) at a wavelength $\lambda = 0.85$ μm (the Verdet constant is $V = 2$ rad m$^{-1}$ T$^{-1}$) we obtain a value $3.25\times10^{-2}$ deg h$^{-1}$. According to experimental work [261], the action of terrestrial magnetic field in the case of an isotropic-fiber gyroscope gives the same value of phase difference as the Earth rotation (15 deg h$^{-1}$). The ways of reducing the effect of magnetic field are evident from expressions (21) and (22) — strengthening linear birefringence, reducing circular birefringence (fiber torsion) and its asymmetry with respect to the middle of the fiber circuit, and increasing the wavelength, since $V \sim 1/\lambda^2$. The use of a depolarizer in the FRI circuit was proposed in Refs [186, 268] for reducing the magnetic effects on the FRI zero drift. However, this proposal is supposedly faulty. A comparison between expressions (4) and (21) shows that the ratio between the counterpropagating-wave phase differences related to the Faraday and Sagnac effects for an FRI decreases with circuit length as $1/\sqrt{L}$, given the magnetic field, fiber parameters, and winding radius. This signifies that the relative magnetic responsivity becomes lower with increasing a number of turns. On the strength of relationship (19), the use of an anisotropic fiber with a purely linear birefringence could seemingly solve the problem of magnetic responsivity. However, the circular component in fiber birefringence can hardly be eliminated in real fibers due to accidental twists arising in the course of pulling fiber and fiber winding around a coil [174].

### 5.6 Nonreciprocal effects associated with the nonlinear interaction of counterpropagating waves (optical Kerr effect)

The fifth group ($\Phi_5$) of additional signals at the FRI output is made up of nonreciprocal nonlinear effects emerging when the counterpropagating wave intensities are different. These effects are related to the dependence of the fiber refractive index on the optical radiation intensity [269], which is governed by the nonlinear optical Kerr effect. The magnitude of the effect depends on the value of quadratic nonlinearity of the refractive index $\chi_3$ for the light-guiding fiber core material and is related to the high optical power density in the single-mode fiber owing to a small core diameter (4–8 μm). These effects in FRIs were considered in Refs [76, 77, 270–273].

We consider below the case when the polarizations of counterpropagating waves are collinear, but their intensities are different. An analysis of counterpropagating-wave

propagation through a nonlinear medium, performed in Ref. [23], in this instance reveals that the intensity dependence of the SMF refractive index is combined from three terms:

$$\delta n^{\pm} = \frac{\chi_3}{2n}\left(|E^{\pm}|^2 + |E^{\mp}|^2 + |E^{\mp}|^2\right). \quad (24)$$

The first term in formula (24) relates to the self-saturation of the wave $|E^{\pm}|^2$, the second term with the saturation by the counterpropagating wave $|E^{\mp}|^2$, and the third, equal to the second one, with the cross-saturation.

The cross-saturation owes its nature to the fact that counterpropagating waves produce a standing structure, which 'writes' by virtue of the nonlinear Kerr effect a virtual multilayer mirror in the medium, with the consequential reflection of the counterpropagating waves [274 – 277]. The first two nonlinear terms in the refractive index of the glass fiber core material prove to be equal for oppositely directed waves even when their intensities are different and do not produce nonreciprocity. The third term associated with multiple reflection of refractive index from the nonlinear mirror proves to be responsible for the occurrence of a nonreciprocal nonlinear phase difference at the FRI output, which is defined by the distinction $\Delta P$ between powers of the counterpropagating waves and the nonlinear polarizability $\chi_3$:

$$\Delta n \sim \chi_3\left[|E^{+}|^2 - |E^{-}|^2\right] \sim \chi_3\,\Delta P\,.$$

These effects may be substantially weakened through the utilization of low-coherence broadband radiation sources. For them, the standing structure of refractive index, essential for the emergence of nonreciprocity, coincides for different radiation wavelengths only over a coherence length $l_{\rm coh} = \lambda^2/\Delta\lambda$ near the middle of the fiber circuit [278 – 280]. In this case, $\Phi_5 = k\Delta P\, l_{\rm coh}$ (for quartz SMFs, one has $k = 2\times 10^5$ rad $\mu$W$^{-1}$ [23]). The FRI output rotation rate (expressed in units of deg h$^{-1}$) equivalent to $\Phi_5$ is $\Delta\Omega_5 \approx 10^5\ \lambda c\,\Phi_5/(\pi L D)$ and decreases in proportion to the diameter and length of the circuit. Numerical estimates performed in Ref. [281] in accordance with the expression for nonlinear nonreciprocal FRI effects give a value of $\Delta\Omega_5 = 2\times 10^{-5}$ deg h$^{-1}$ for $P = 100$ mW, $\Delta P = 0.02$ mW, $D = 1$ m, $L = 5$ km, $\lambda = 1.55$ $\mu$m, and $\Delta\lambda = 15$ nm.

The placement of a polarizer has no effect on the FRI zero shift related to the Kerr effect. When counterpropagating waves with a variable or fluctuating amplitude differ in intensity, the nonlinear effects in an FRI can, because of asymmetry in the opposite directions, give rise to transient effects at the modulation frequency, which are similar to those considered in Section 5.4 [282]. Possibilities for eliminating multiple reflections from the virtual mirror have been considered in the scientific literature. These include high-frequency modulation of the fiber length in the middle of the circuit [23] or breaking the fiber in the middle of the circuit [281] with the aim of making an air gap at the place of formation of the field standing structure. So far these techniques have not found practical use.

In resonator FOGs, the nonlinear optical Kerr effect may change the resonance frequency and give rise to bistability [283].

When the counterpropagating waves have different polarizations (are noncollinear), additional nonlinear, nonreciprocal polarization effects may occur, which are related to the variation of polarization of each wave owing to the action of the noncollinear counterrunning wave. The change of polarization of each of the counterpropagating waves may occur due to nonlinear anisotropy induced by the action of intensity of the differently polarized counterrunning wave. This effect is independent of the spectral width of the radiation source and is accumulated over the entire circuit length. Furthermore, the polarization of one of the waves will change due to the multiple reflection of the differently polarized counterrunning wave from the virtual nonlinear mirror, which comes about from the Kerr effect on the standing structure of the counterrunning waves. The localization of this effect along the circuit depends on the coherence properties of the radiation source. These two nonlinear polarization effects for noncollinear counterrunning waves are different in nature and have come to be known in the scientific literature as the Hänsch effect [284, 285] and the Yakubovich effect [286]. More recently they were discussed in considerable detail in Refs [274 – 277]. Numerical estimates of the nonlinear effects and the phase nonreciprocity for noncollinear waves in FRIs are given in paper [270]. It is pertinent to note that the nonlinear optical Kerr effect may lead to the depolarization of nonmonochromatic radiation at the output of weakly anisotropic SMFs due to induced anisotropy, when the radiation polarization state at the input is differed from the polarization of SMF eigenmodes [287]. Notice that the occurrence of a frequency difference among counterrunning waves in a ring laser, associated with the Hänsch effect, was earlier considered in Refs [288 – 290].

### 5.7 Nonreciprocity associated with relativistic effects in fiber gyroscopes

First of all it should be remembered that the Sagnac effect is relativistic by itself [48 – 52] and, as shown in works [48, 52], is a consequence of the relativistic law of velocity composition — the linear velocity of interferometer rotation and the phase velocities of each of the counterpropagating waves, which is reflected in formula (3). Notice that expression (3) is valid in the absence of angular acceleration and spatially nonuniform static gravitational field. Their influence on the Sagnac effect was considered in Refs [291, 292].

We now turn to a consideration of the influence of gravity-related relativistic effects on the phase difference of counterpropagating waves in an FRI and, hence, on the FOG output signal.

When a gravitational field is produced by a rotating mass, the Lense – Thirring effect is bound to occur, which is a GTR effect [293]. Until the present time this effect has not been revealed experimentally. It is a gravitational analogue of electromagnetic induction and has the effect that a rotating mass located at the center of the interferometer exerts a different action on the phases of waves travelling in the direction of mass rotation or in the opposite direction. As far back as 1921, to record this effect from the Earth's rotation, Silberstein [294] proposed the use of a ring interferometer, in which the effect under consideration should produce an additional phase difference among counterrunning waves. In this case, hopes were being pinned on a ring interferometer measuring 630 m $\times$ 340 m, which was being designed by Michelson and his coworkers at that time. However, its sensitivity proved to be clearly not high enough for revealing the Lense – Thirring effect. Shortly after the advent of the first FRIs, Scully et al. [295] proposed the use of large-sized FRIs for recording the Lense – Thirring effect and also for the high-precision verification of the main postulate of the STR — the isotropy of the velocity of light.

Specific requirements on FRI parameters for these experiments were considered in papers [125, 127], where it was shown, in particular, that the attainment of the requisite sensitivity necessitated constructing an FRI several kilometers in diameter. The main difficulty here lies in the fact that the phase difference of counterpropagating waves due to the Lense – Thirring effect is extremely small and may escape detection against the noise background of the receiving equipment and the background of other nonreciprocal effects considered above. The rotation of an FRI several kilometers in diameter stationed on the Earth is impossible to eliminate, while the phase difference of counterpropagating waves, expected from the Lense – Thirring effect, is eight orders of magnitude lower than that from the Sagnac effect related to the Earth's rotation. That is why the weak effect will have to be observed against the background of a very strong one, making the observations extremely difficult. Recently, for the observation of the Lense – Thirring effect, Tartaglia [296] proposed the use of a ring interferometer with a dimension greater than the Earth's perimeter, for which purpose the interferometer mirrors would be stationed on artificial Earth satellites.

Gravitational waves can also give rise to a phase difference of FRI counterpropagating waves. To detect them by optical techniques, a Michelson interferometer with 4-km long arms is now in the making in the framework of the LIGO Project in the USA. As an alternative to the LIGO Project, a discussion in the scientific literature is now underway concerning the possibility of using a special-design FRI to stage basic experiments on measuring gravitational waves [297]. The idea of this experiment consists in the following. When binary stars rotate, gravitational radiation rotating in time arrives at the Earth (see Fig. 7). In relation to the phase of the gravitational radiation, the photons of light will change their frequency along the perimeter of the FRI fiber circuit: 'redden' or 'get blue', but on average the phase incursion will be zero. For this not to take place, the velocity of light along the perimeter of one of the counterrunning waves should be equal to the rotational velocity of the gravitational wave. Then, the photons in this direction of light propagation will periodically 'get blue' and 'redden'. In the opposite direction of light propagation, this velocity synchronization does not take place, since the photons of this wave go counter to the rotation of the gravitational radiation. The phase difference of the counterrunning waves at the interferometer output will change in time with the rotational frequency of the gravitational wave field. Estimates show that attaining velocity synchronization of the light and gravitational waves for a rotational frequency of the gravitational field of about 10 kHz requires that the fiber ring diameter should be about 13 km (a fiber length of 41 km). In this case, the expected phase difference estimated by the authors of this project will exceed the FRI sensitivity threshold. To reduce the diameter of such an FRI, Kingsley [297] proposed the employment of a system slowing down the photon velocity due to a fiber of requisite length wound over a toroid, whose diameter would define the dimension of the gravitational ring interferometer. However, high radiation energy losses arise for so high a rotational frequency (10 kHz) of the binary star, resulting in its rapid collapse and a strongly limited time of observation of the gravitational waves.

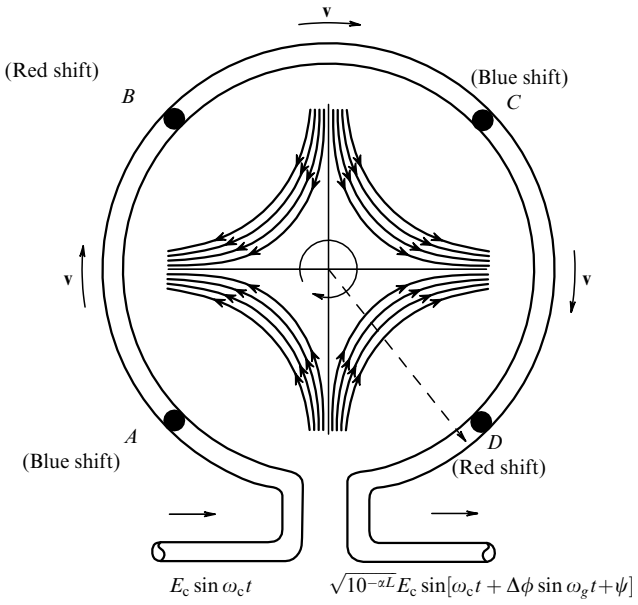


**Figure 7.** Sagnac interferometer for measuring gravitational waves [297]. The propagation direction and velocity $v$ of one light wave coincides with the sense of rotation of a gravitational wave, whose circular frequency is $\omega_g$; $\omega_c$ is the circular frequency of light; $\alpha$ is the SMF light absorption coefficient; $E_c$ is the electric field amplitude of the light wave at the input of the fiber circuit, and $\psi$ is the phase of the wave. For clarity, the full circles stand for the photons which change their energy (frequency) to the greatest degree under the action of the gravitational field.

We note that also discussed in the scientific literature is the possibility of recording gravitational waves employing, along with FRIs, polarization ring interferometers on the basis of discrete optical elements [298 – 300] which were first proposed in Refs [301, 302]. In these interferometers, a polarization prism fulfils the function of a beam splitter at the ring input, with the effect that counterpropagating waves have mutually orthogonal polarizations. A fiber version of polarization interferometers (PFRIs) may possess a high responsivity due to a large circuit length.

Because the Sagnac effect is, in accordance with expression (3), inversely proportional to the wavelength, it is advantageous to go over to shorter-wavelength radiation, including the employment of de Broglie waves of material particles with a nonzero mass at rest (electrons, neutrons, atoms, etc.). For material particles possessing spin, which follow a curvilinear path, there occurs a relativistic kinematic effect termed *Thomas precession* [303 – 308]. It consists in the fact that the spin of a particle which describes a curvilinear path is rotated (exhibits precession). If material particles (for instance, electrons) have a similar spin orientation (similar polarization) at the input of a ring interferometer, the spin orientations of counterpropagating waves will be different at its output. In the interference between the counterpropagating waves this will give rise to a phase difference unrelated to rotation [309, 310], whose order of magnitude is defined by the ratio $v^2/c^2$. To eliminate the effect of Thomas precession on the de Broglie-wave ring interferometers, Malykin [49] proposed the use of material particles with a zero spin value — $\pi$-mesons. For optical ring interferometers, the Thomas precession will not change the state of light polarization, since the polarization of a single photon is always circular' — right or left. In other words, the spin of a photon as a particle with a zero rest mass can only be aligned with or opposed to the direction of motion, which is the preferred one for the photon because there exists no rest frame for it [311].

Therefore, the photon spin orientation cannot change with respect to the direction of motion. This result can be explained in a different way. As shown in Refs [306, 307], for a particle velocity $v = c$ its spin turns by one revolution per revolution of the particle. Therefore, when the photon travels through a ring interferometer its spin turns by 360° and thereby reverts to the initial state. When there exists an optical medium with a refractive index $n$ in the interferometer (like, for instance, in an FRI), the photons nevertheless travel in it with the velocity of light and the $n$-fold moderation of the average velocity is attributable to the reemission-related delay.

The main c o n c l u s i o n of this section is as follows. Relativistic effects (owing to their smallness) can hardly affect the measurement accuracy of orientation and navigation FOGs. On the other hand, large-sized FRIs can be employed to discover these effects.

## 6. Fluctuations and ultimate sensitivity of fiber gyroscopes

The FOG sensitivity determined by noise of different origins at the photodetector output ($\Phi_7$) was considered in Refs [95, 312 – 326]. Several sources make contributions to the noise: quantum (shot) noise related to the discrete nature of photons and photoelectrons; the natural noise of a radiation source, related to the beats of spectral components [95, 316, 319] that emerge during quadratic detection (photoreception) of the optical spectrum; equilibrium thermal fluctuations of the SMF refractive index [313, 324], which modulate the counter-running wave radiation; fluctuations associated with light scattering, and flicker noise related to the passage of feed current through a semiconductor radiation source. These constituents are different in level with and without phase modulation, because modulation gives rise to additional noise components at the modulation frequency owing to beats of noise components (during photoreception) at frequencies corresponding to the first and second harmonics of the modulation frequency [320, 321].

The respective spectral densities of noise modulation of the photocurrent at the FRI output, caused by shot noise and the natural noise of a radiation source, are [95, 316, 318]

$$\overline{m_1^2} = \frac{2e}{i_0}\,, \qquad \overline{m_2^2} = \frac{1}{\Pi}\,,$$

where $e$ is the electron charge, $\Pi$ is the spectral band of the radiation source, $i_0 = \gamma P$ is the constant constituent of the current, $P$ is the optical power, and $\gamma$ is the quantum efficiency of the photodetector.

The depth of chaotic modulation of the natural fluctuations of the radiation source does not, unlike shot noise, depend on the magnitude of the photocurrent at the FRI output and is determined only by the bandwidth $\Pi$ of the radiation source. For a Gaussian or Lorentzian line shape, the depth of modulation of radiation source fluctuations varies insignificantly (up to a factor of 1.5) in comparison with the $\Pi$-like line shape. The thermal fluctuations of refractive index, which may be responsible for additional noise modulation $\overline{m_3^2}$ of the photocurrent at the FRI output, were considered in Refs [313, 326]. The level of thermal equilibrium fluctuations of the SMF refractive index and their dependence on the fiber length was experimentally investigated with the use of a Mach – Zehnder interferometer by Wanser [327]. It was shown in the work cited that the spectral density of phase fluctuations at the fiber output, related to the equilibrium fluctuations of refractive index, is proportional to the fiber length and the temperature squared, and inversely proportional to the wavelength and the mode diameter. These dependences show the way to reducing thermal phase fluctuations, in particular, by lowering the circuit temperature. The spectral density of thermal phase fluctuations at the output of a 1-km long fiber segment, measured in Ref. [327], was equal to 2 μrad $\mathrm{Hz}^{-1/2}$.

The influence of equilibrium fluctuations of the refractive index on the output FOG signal has a specific feature which consists in that their effect is stronger for fiber sections remotest from the middle of the fiber circuit (see Section 5.4). Furthermore, falling into the reception band at the modulation frequency are only those low-frequency perturbations whose frequency does not exceed the reception bandwidth. These issues were treated in Refs [324, 325]. The results of the experimental work [324] on the revelation of the effect of equilibrium refractive-index fluctuations on the FOG signal are not convincing enough and invite further refinements. The Rayleigh scattering, which is the principal cause of optical energy loss in modern SMFs, changes the constant constituent of photocurrent and thereby changes the magnitude of shot noise. Furthermore, arriving at the output is the radiation coherent with counterpropagating waves, which is scattered from fiber segments with lengths equal to the coherence length and located at the center of the fiber ring and at its ends. This part of the scattered radiation can introduce an additional correction to the phase of the rotation signal. The radiation scattered from the remaining portions of the fiber circuit is incoherent with counter-propagating waves. It will give rise to an additional noise interference signal [328] whose intensity is defined by the product of the fields of the principal and scattered waves. This part of the scattered radiation may lead to the occurrence of additional noise modulation $\overline{m_4^2} < \overline{m_2^2}$ in the output signal. Modulation estimates for a superluminescence diode give an FRI zero drift to an order of $10^{-6}$ deg $\mathrm{h}^{-1}$. The flicker current fluctuations are hard to predict, since they are largely dependent on the production technology of a radiation source and may vary from sample to sample.

The rotation sensitivity threshold is determined from the condition that the signal-to-noise ratio at the photodetector output in a given reception band be equal to unit. Following the results of Ref. [95], the threshold rotational velocity $\Omega_{\mathrm{thres}}$ (when using the modulation measuring technique from the first harmonic of the modulation frequency and the optimal amplitude of phase modulation corresponding to the peak of the first-order Bessel function) may be written as

$$\Omega_{\mathrm{thres}} = \frac{1.57\lambda c}{2RL}\sqrt{\left(\overline{m_1^2} + \overline{m_2^2} + \overline{m_3^2} + \overline{m_4^2}\right)\Delta F}\,, \tag{25}$$

where $\Delta F$ is the reception band. Considering that $\overline{m_1^2}$, $\overline{m_2^2} > \overline{m_4^2}$ and the $\overline{m_3^2}$ value can be lowered by lowering the SMF temperature, we conclude that the shot noise $\overline{m_1^2}$ and the noise of a superluminescence radiation source $\overline{m_2^2}$ make the main contribution to the sensitivity threshold. In this case, by raising the output power it is possible to improve the ultimate sensitivity as long as the shot-noise modulation depth ($\overline{m_1^2} = 2e/i_0$) exceeds the modulation depth of the radiation source noise ($\overline{m_2^2} = 1/\Pi$). As the current is further increased, the sensitivity threshold ceases to depend on the photocurrent, because the noise related to the natural fluctuations in the radiation source comes to be dominant at the FRI output. This noise can be significantly reduced if it is compensated

for. To this end it is possible to use a fraction of the initial source power [81, 324, 325, 329]. During propagation through the entire length of the fiber circuit, the useful signal acquires an additional phase. That is why an additional phase should also be introduced into the compensation signal, employing a delay line or some other device. As shown by subsequent investigations [321], it was not the amplitude of phase modulation $\Phi_m = 1.8$ rad, corresponding to the peak of the first harmonic in the photocurrent, that turned out to be optimal for increasing the signal-to-noise ratio, but $\Phi_m = 2.7$ rad, corresponding to the minimum of the constant component of the photocurrent.

The techniques which make it possible to obtain a linear dependence between the angular rotational velocity and the output signal over a wide range of angular velocities under measurement were considered in Refs [258, 330–351], and those involving measurements of the entire set of modulation frequency harmonics in the photocurrent were examined in Refs [331, 335, 339, 344–346]. The possibility of using the heterodyne technique was explored in Refs [349–351]. In some cases, the employment of these techniques allows an improvement in sensitivity, which was demonstrated in paper [88]. We note that the variation of the level of fluctuations may in some cases serve the purpose of rotation indication [352].

In the previous sections we considered the causes for the occurrence of additional signals at the FRI output. Taking into account these signals, the resultant phase difference $\Phi_\Sigma$ at the FRI output may be written as

$$\Phi_\Sigma = \Phi_S + \Phi_1 + \Phi_2 + \Phi_3 + \Phi_4 + \Phi_5 + \Phi_6 + \Phi_7 . \qquad (26)$$

One can see from expression (26) that the output signal can contain, along with the rotation signal ($\Phi_S$) and the noise signal ($\Phi_7$), signals related to light scattering ($\Phi_1$), polarization ($\Phi_2$) and transient ($\Phi_3$) effects, imposition of magnetic field ($\Phi_4$), and nonlinear ($\Phi_5$) and relativistic ($\Phi_6$) effects. When the additional signals are stable, it is possible to subtract them during data processing. When they vary with time, they determine the drift of the signal and the measurement error of angular velocity.

Therefore, the fluctuations of the signal at the FOG output determine the ultimate sensitivity; the magnitude of the sum of additional signals in the absence of rotation determines the permanent 'pedestal', while its variation (including temperature ones) governs the drift of the FOG signal.

## 7. Application of fiber gyroscopes and fiber ring interferometers

In this section we discuss the application of FRI-based FOGs intended for measurements of rotational velocity and rotation angle as well as diversified uses of FRIs unrelated to the rotation of an object, including their use as acoustic sensors [353] or hydrophones [354, 355]. By now fiber-optic gyroscopes (FOGs) have entered the stage of batch production and have occupied a rather big niche among medium-precision gyroscopic instruments. The sensitivity range of optical fiber gyroscopes is rather broad: from 100 deg $h^{-1}$ to 0.005 deg $h^{-1}$. The 'minimal scheme' [85] with one polarizer (see Fig. 5) underlies batch-produced instruments. The elemental base of the batch-produced instruments is quite diversified. Some companies use traditional welded or polished fiber-optic elements (fiber modulators and polarizers, welded or polished beam splitters), whereas the others resort to integrated optical elements or modules, on which a modulator, a beam splitter, and a polarizer are mounted. Either semiconductor superluminescence emitters or superfluorescence active-fiber emitters serve as FOG radiation sources. On the not nearly complete list of companies involved in the batch production of fiber gyroscopes in the USA are Honeywell, Litton Corp., KVH Inc., Fibersense Technology Corp., and Andrew Kintec Corp.; in Europe are Photonetics, SFIM, Litef, and IMAR; in Africa is CSIR; in Japan are Communications Research Laboratory and Tamagawa, and in Russia are the NTK 'Fizoptika' (Moscow) and 'Korpus' (Saratov), the Instrument-Making Scientific-Production Unit (Perm') and some others. FOGs have a rather broad area of practical application for the purposes of gyroscopy, orientation, and navigation [13, 356–361]. FOGs are employed in ground transportation vehicles, among which are automobiles, electric cars, robots, and different agricultural machines which should move according to a preassigned program [361]. These gyroscopes have a sensitivity to an order of 10 deg $h^{-1}$. In taxis and police cars they are employed when moving along prespecified routes, including those in megalopolises. The length of straight portions covered when pursuing the route is determined by integrating velocity, and the turn through a given angle is checked by integrating the FOG signal. For objects executing nonplanar motion (including helicopters and rockets), to determine the orientation in space advantage is taken of triaxial devices containing three independent angular rotation sensors with mutually orthogonal axes. Moreover, FOGs are employed when laying railways and drilling wells. In this case, the gyroscope axis is placed perpendicular to the rail or the drill. As the gyroscope moves along the railway or advances with the drill end, the gyroscope reveals the axis rotations, i.e. departures from the rectilinear path. FOGs are also predicted soon to start occupying the niche of navigational gyroscopes, which has previously belonged to laser and mechanical gyroscopes.

FRIs can also be used as conventional phase sensors of variable action. This is possible when the sensor is located at one of the ends or the sensing function is fulfilled by a portion of the fiber at one of the ends of the circuit. As noted above, under an asymmetric action on the circuit SMF there appears the second harmonic of the signal in the interference signal at the FRI output. This kind of sensor is a quadratic detector with a low responsivity to weak disturbances. However, a linear response can be obtained on introducing additional modulation $\Omega_m$. In this event, the signal is observed not at the disturbance frequency $\Omega_{inf}$, but at frequencies $\Omega_m \pm \Omega_{inf}$, and the characteristic of the fiber sensor is defined by the first-order Bessel function whose argument is equal to

$$\Phi_{inf} \sin \Omega_{inf} \frac{(L - L_{inf})\, n}{2c} ,$$

i.e. depends on the level, frequency, and localization of the signal in the fiber coil $L_{inf}$. The highest sensor sensitivity [191] for a given frequency of the signal is defined by the condition

$$\sin \Omega_{inf} \frac{(L - L_{inf})\, n}{2c} = 1 .$$

This relationship implies that the sensor is insensitive to constant actions and has a nonuniform frequency response. An advantage of ring sensors over the Mach–Zehnder and Michelson schemes is that the interfering waves travel along similar paths.

FRIs are also employed for measuring the flow velocity of liquids [362]. To do this requires providing a contact of the flow with the light-guiding core throughout some segment of the fiber circuit, which will give rise to nonreciprocity effects in the FRI due to emerging the Fresnel – Fizeau liquid flow entrainment.

Furthermore, presently under discussion are issues related to the application of FRIs and PFRIs in physical experiments, including the detection of various nonreciprocal effects in different media, occurring under the action of magnetic fields of different configurations [363, 364]. Chow et al. [365] considered the possibility of applying FRIs to the solution of several geophysical problems. De Carvalho and Blake [366] employed an FRI to measure the Lorentzian addition to the Fresnel – Fizeau entrainment coefficient. The first attempts to take measurements of this kind were made by Harress as far back as 1909 [34].

Nullifying the effects of asymmetric modulation in an FRI at the frequencies that satisfy the condition

$$\omega\tau = \frac{\omega L \Delta n}{c} = \pi$$

can be used for measuring the chromatic dispersion [367, 368] and the polarization mode dispersion [369] in an SMF and for measuring the dependence of an SMF nonlinear refractive index on the light intensity [370]. FRIs are also used for contactless profile monitoring of optical surfaces [371, 372]; as current [373 – 377] and electric field [378] sensors, magnetometers [379], and tension sensors [380]; for measuring the extinction coefficient of fiber polarizers [381]; as optical frequency filters [238, 239], temperature sensors [382, 383], optical switches [384 – 388], and optical hydrophones [354, 355], and also for measuring the velocity of object motion from the Doppler effect [389]. FRIs also find a series of other interesting applications [390 – 402].

Also discussed in the scientific literature is the feasibility of using special-design FRIs for staging basic experiments to discover STR and GTR effects, including experiments to measure gravitational waves [297], and also the Lense – Thirring effect and the assumed anisotropy of the velocity of light [295]. These experiments were conceptually considered in Section 5.7.

The military aspects of applications of FRIs were considered in Refs [403 – 406], and Ref. [407] was concerned with the commercial aspects of their use.

We note that a large number of journal papers dedicated to FRIs and published from 1976 to 1989 were collected in Ref. [408].

## 8. Conclusions

It is pertinent to note that fiber gyroscopy has now gone through the stage of purely scientific research and entered the stage of production of gyroscopic devices, primarily those of the medium-precision class (15 – 0.05 deg $h^{-1}$), and it coexists along with more sensitive laser gyroscopy (1 – 0.001 deg $h^{-1}$) intended for navigational purposes, i.e. for the determination of the latitude of a place by measuring the rotational velocity of the Earth.

The development of fiber gyroscopy will follow several directions.

(1) Improvement of the stability of FOGs thanks to improvements in the quality of the elements (modulators, beam splitters, polarizers, and fiber circuits) and their temperature stability; improvement of the methods for checking the mutual alignment of the elements during assembly, and also development of designs insensitive to mechanical and acoustic vibrations and temperature gradients.

(2) Improvement of the ultimate sensitivity by lowering the modulation depth of radiation source fluctuations. This is possible in the path of raising the intensity and broadening the band of radiation sources [223]. Raising the sensitivity and stability may have the effect that fiber gyroscopes will oust laser ones from their place in navigational gyroscopy.

(3) Lowering the cost and miniaturization of the devices through the batch production of integrated modules, which would substantially enlarge the demand for medium-precision (to 1 deg $h^{-1}$) orientation gyroscopes.

(4) Further investigation of the possibility of designing lengthy high-sensitivity FRIs with the aim of using them for basic experiments, including the field of gravitational wave detection and studies of the effects of special and general relativity theory.

As noted above, resonance fiber gyroscopy has not gained wide acceptance to date. However, it may well be that the change-over from laser sources to broadband superluminescence radiators will serve as an impetus to its future development. Experiments conducted in this field have been reported in the scientific literature [409 – 411]. The advantages of these schemes over the traditional ones are discussed, and quite optimistic estimates are given [412 – 414]. Moreover, it is not impossible that the development of resonance gyroscopy will take a different path: involving not multiturn fiber coils, but high-$Q$ integrated optical resonators, because the shift of resonance frequencies for counterpropagating waves is independent of the length of the resonator perimeter.

Along with optical gyroscopes, the feasibility of developing gyroscopic instruments on the basis of the Sagnac effect for waves quite different in nature and from different frequency ranges is also considered in the scientific literature. Since the Sagnac effect is inversely proportional to the wavelength, the sensitivity can be expected to rise with decreasing wavelength. Sagnac-effect measurements have been reported for X-ray waves [42], de Broglie waves of electrons [40], neutrons [43], and different atoms [44 – 46]. However, at the moment new proposals cannot (owing to the complexity of their realization) seriously compete with optical gyroscopy.

**Acknowledgments.** In conclusion the authors express their gratitude to V N Logozinskiĭ for a series of helpful consultations, to Yu A Kravtsov and Vl V Kocharovskiĭ for discussing the issues related to the impact of the Rytov phase on FRI operation, to Yu A Mamaev for his assistance in gleaning the publications, and to M N Kucheva for her aid in designing the manuscript.

This work was supported in part by the Russian Foundation for Basic Research (grants 00-15-96732 and 00-02-17344).

## References

1. Bershteĭn I L *Dokl. Akad. Nauk SSSR* **75** 635 (1950)
2. Wallace A "Electromagnetic wave gyroscopes or angular velocity measuring system", US Patent N 3102953 (Sept. 3, 1963, filed Jul. 9, 1958)
3. Vali V, Shorthill R W *Appl. Opt.* **15** 1099 (1976)
4. Vali V, Shorthill R W *Appl. Opt.* **16** 290 (1977)

5. Lin S-C, Gialorenzi T G *Appl. Opt.* **18** 915 (1979)
6. Ezekiel S, Arditty H J, in *Fiber-Optic Rotation Sensors and Related Technologies: Proc. of the 1st Intern. Conf. MIT, Cambridge, Mass., USA, November 9–11, 1981* (Springer Ser. in Optical Sciences, Vol. 32, Eds S Ezekiel, H J Arditty) (Berlin: Springer-Verlag, 1982) p. 2
7. Arditty H J, in *Fiber-Optic Rotation Sensors and Related Technologies: Proc. of the 1st Intern. Conf. MIT, Cambridge, Mass., USA, November 9–11, 1981* (Springer Ser. in Optical Sciences, Vol. 32, Eds S Ezekiel, H J Arditty) (Berlin: Springer-Verlag, 1982) p. 44
8. Savel'ev A N, Solov'eva T I *Zarubezhnaya Radioelektronika* (6) 55 (1982)
9. Böhm K et al. *Radio Electron. Eng.* **753** 121 (1983)
10. Bergh R A, Lefevre H C, Shaw H J *J. Lightwave Technol.* **LT-2** 91 (1984)
11. Pavlath G A, Suman M C *Navigation: J. Inst. Navigation* **31** 70 (1984)
12. Culshaw B, Giles I P *J. Phys E: Sci. Instrum.* **16** 5 (1983)
13. Kuritsky M M, Goldstein M S *Proc. IEEE* **71** 1156 (1983) [Translated into Russian *TIIER* **71** (10) 47 (1983)]
14. Burns W K *Laser Focus* **20** 83 (1984)
15. Lefevre H C et al. *Proc. SPIE* **719** 101 (1986)
16. Sheremet'ev A G *Volokonnyĭ Opticheskiĭ Giroskop* (Fiber-Optic Gyroscope) (Moscow: Radio i Svyaz', 1987)
17. Cahan F, Jones E *Int. Mech. Eng.* **58** 113 (1987)
18. Dianov E M et al. *Tr. Inst. Obshch. Fiz. Akad. Nauk SSSR* **15** 140 (1988)
19. Baĭborodin Yu V, Mashchenko A I *Zarubezhnaya Radioelektronika* (3) 95 (1988)
20. Sidorova R A *Zarubezhnaya Radioelektronika* (11) 89 (1988)
21. Brown A D et al. *Electrotechnology* (Jan.) 17 (1989)
22. Lefevre H C, in *Optical Fiber Sensors* Vol. 2 *Systems and Applications* (Eds B Culshaw, J Dakin) (Boston: Artech House, 1989) p. 381
23. Lefevre H *The Fiber-Optic Gyroscope* (Boston: Artech House, 1993)
24. Okosi T et al. *Volokonno-Opticheskie Datchiki* (Optical Fiber Sensors) (Ed. T Okosi) [Translated from Japanese (Moscow: Energoatomizdat, 1990)]
25. Lefevre H C *Proc. SPIE* **2837** 2 (1996)
26. Vavilov S I "Eksperimental'nye Osnovaniya Teorii Otnositel'nosti" ("Experimental Foundations of the Relativity Theory"), in *Collected Works* Vol. 4 (Moscow: Izd. AN SSSR, 1956) p. 9
27. Zernike F *Physica* **13** 279 (1947)
28. Post E J *Rev. Mod. Phys.* **39** 475 (1967)
29. Hariharan P *Appl. Opt.* **14** 2319 (1975)
30. Anderson R, Bilger H R, Stedman G E *Am. J. Phys.* **62** 975 (1994)
31. Malykin G B *Usp. Fiz. Nauk* **167** 337 (1997) [*Phys. Usp.* **40** 317 (1997)]
32. Lodge O *Philos. Trans. R. Soc. London Ser. A* **184** 727 (1893)
33. Michelson A A *Philos. Mag. Ser. 6* **8** 716 (1904)
34. Harress F "Die Geschwindigkeit des Lichtes in bewegten Körpern", Dissertation (Jena, 1912)
35. Sagnac M G *C.R. Acad. Sci.* **157** 708 (1913)
36. Sagnac M G *C.R. Acad. Sci.* **157** 1410 (1913)
37. Sagnac M G *J. Phys.* (Paris) **4** 177 (1914)
38. Michelson A A *Astrophys. J.* **61** 137 (1925)
39. Michelson A A, Gale H G, Pearson F *Astrophys. J.* **61** 140 (1925)
40. Hasselbach F, Nicklaus M *Phys. Rev. A* **48** 143 (1993)
41. Rosenthal A *J. Opt. Soc. Am.* **52** 1143 (1962)
42. Vysotskiĭ V I et al. *Usp. Fiz. Nauk* **164** 309 (1994) [*Phys. Usp.* **37** 289 (1994)]
43. Werner S A, Staudenmann J-L, Colella R *Phys. Rev. Lett.* **42** 1103 (1979)
44. Riehle F et al. *Phys. Rev. Lett.* **67** 177 (1991)
45. Lenef A et al. *Phys. Rev. Lett.* **78** 760 (1997)
46. Gustavson T L, Bouyer P, Kasevich M A *Phys. Rev. Lett.* **78** 2046 (1997)
47. Newburgh R G et al. *Proc. IEEE* **62** 1621 (1974) [Translated into Russian *TIIER* **62** (12) 6 (1974)]
48. Vugal'ter G A, Malykin G B *Izv. Vyssh. Uchebn. Zaved., Radiofiz.* **42** 373 (1999)
49. Malykin G B *Izv. Vyssh. Uchebn. Zaved., Radiofiz.* **41** 767 (1998)
50. Landau L D, Lifshitz E M *Teoriya Polya* (The Classical Theory of Fields) (Moscow: Nauka, 1967) [Translated into English (Oxford: Pergamon Press, 1975)]
51. Logunov A A, Chugreev Yu V *Usp. Fiz. Nauk* **156** 137 (1988) [*Sov. Phys. Usp.* **31** 861 (1988)]
52. Malykin G B *Usp. Fiz. Nauk* **170** 1325 (2000) [*Phys. Usp.* **43** 1229 (2000)]
53. Ezekiel S, Balsamo S R *Appl. Phys. Lett.* **30** 478 (1978)
54. Macek W M, Davis D T *Appl. Phys. Lett.* **2** 67 (1963)
55. Privalov V E, Fridrikhov S A *Usp. Fiz. Nauk* **97** 377 (1969) [*Sov. Phys. Usp.* **12** 153 (1969)]
56. Pomerantsev N M, Skrotskiĭ G V *Usp. Fiz. Nauk* **100** 361 (1970) [*Sov. Phys. Usp.* **13** 147 (1970)]
57. Aronowitz F, in *Laser Applications* Vol. 1 (Ed. M Ross) (New York: Academic Press, 1971) p. 133 [Translated into Russian (Moscow: Mir, 1974) p. 182]
58. Wilkinson J R *Prog. Quant. Electron.* **11** 1 (1987)
59. Kravtsov N V, Kravtsov N N *Kvantovaya Elektron.* **27** 98 (1999) [*Quantum Electron.* **29** 378 (1999)]
60. Stedman G E *Rep. Prog. Phys.* **60** 615 (1997)
61. Dunn R W *Appl. Opt.* **37** 6405 (1998)
62. Rowe C H et al. *Appl. Opt.* **38** 2516 (1999)
63. Denisov V I et al. *Kvantovaya Elektron.* **26** 171 (1999) [*Quantum Electron.* **29** 171 (1999)]
64. Brown R B, NRL Memorandum Report N1871 (Washington, DC: Naval Research Lab., 1968)
65. Alekseev E I et al. *Pis'ma Zh. Tekh. Fiz.* **10** 443 (1984)
66. Bazarov E N, Semenov A T *Kvantovaya Elektron.* **11** 775 (1984) [*Sov. J. Quantum Electron.* **14** 522 (1984)]
67. Alekseev E I et al. *Kvantovaya Elektron.* **11** 2151 (1984) [*Sov. J. Quantum Electron.* **14** 1436 (1984)]
68. Gur'yanov A N et al. *Pis'ma Zh. Tekh. Fiz.* **11** 321 (1985) [*Sov. Tech. Phys. Lett.* **11** 132 (1985)]
69. Gur'yanov A N et al. *Radiotekhnika* (7) 83 (1987)
70. Andreev A Ts et al. *Zh. Tekh. Fiz.* **63** (1) 116 (1993)
71. Davis J L, Pondrom W L, Thompson D E, in *Fiber-Optic Rotation Sensors and Related Technologies: Proc. of the 1st Intern. Conf. MIT, Cambridge, Mass., USA, November 9–11, 1981* (Springer Ser. in Optical Sciences, Vol. 32, Eds S Ezekiel, H J Arditty) (Berlin: Springer-Verlag, 1982) p. 308
72. Davis J L, Ezekiel S *Opt. Lett.* **6** 505 (1981)
73. Prentiss M G, Davis J L, Ezekiel S, in *Fiber-Optic Rotation Sensors and Related Technologies: Proc. of the 1st Intern. Conf. MIT, Cambridge, Mass., USA, November 9–11, 1981* (Springer Ser. in Optical Sciences, Vol. 32, Eds S Ezekiel, H J Arditty) (Berlin: Springer-Verlag, 1982) p. 297
74. Kotov V M *Kvantovaya Elektron.* **26** 265 (1999) [*Quantum Electron.* **29** 265 (1999)]
75. Oberson P, Huttner B, Gisin N *Opt. Lett.* **24** 451 (1999)
76. Kaplan A E, Meystre P *Opt. Lett.* **6** 590 (1981)
77. Kaplan A E, in *Fiber-Optic Rotation Sensors and Related Technologies: Proc. of the 1st Intern. Conf. MIT, Cambridge, Mass., USA, November 9–11, 1981* (Springer Ser. in Optical Sciences, Vol. 32, Eds S Ezekiel, H J Arditty) (Berlin: Springer-Verlag, 1982) p. 375
78. Sheem S K *Appl. Phys. Lett.* **37** 869 (1980)
79. Burns W K, Moeller R P, Villarruel C A *Electron. Lett.* **18** 648 (1982)
80. Poisel H et al. *Electron. Lett.* **26** 69 (1990)
81. Bukhman A B et al. *Dokl. Akad. Nauk SSSR* **161** 844 (1980)
82. Malykin G B *Opt. Spektrosk.* **76** 540 (1994) [*Opt. Spectrosc.* **76** 484 (1994)]
83. Hotate K et al. *Appl. Opt.* **20** 4313 (1981)
84. Alekseev E I et al. *Pis'ma Zh. Tekh. Fiz.* **5** 1050 (1979)
85. Ulrich R *Opt. Lett.* **5** 173 (1980)
86. McLaughlin D J "Optical gyroscope having means for resolving ambiguities of velocity and direction", US Patent N 3512890 (May 19, 1970, filed Jul. 27, 1965)
87. Kim B Y, Shaw H J *Opt. Lett.* **9** 263 (1984)
88. Bershteĭn I L, Gelikonov V M, Stepanov D P *Izv. Vyssh. Uchebn. Zaved., Radiofiz.* **41** 1461 (1998)
89. Giles I P et al. *Electron. Lett.* **22** 494 (1986)
90. Iwatsuki K, Hotate K, Higashiguchi M *Appl. Opt.* **25** 4448 (1986)
91. Cutler C C, Newton S A, Shaw H J *Opt. Lett.* **5** 488 (1980)
92. Böhm K, Petermann K, Weidel E *Opt. Lett.* **6** 64 (1981)
93. Burns W K, Moeller R P *J. Lightwave Technol.* **LT-1** 381 (1983)
94. Okamoto K et al. *Electron. Lett.* **20** 429 (1984)

95. Andronova I A, Bershteĭn I L *Izv. Vyssh. Uchebn. Zaved., Radiofiz.* **32** 426 (1989)
96. Böhm K et al. *Electron. Lett.* **17** 352 (1981)
97. Alekseev E I et al. *Pis'ma Zh. Tekh. Fiz.* **20** (2) 62 (1994) [*Tech. Phys. Lett.* **20** 74 (1994)]
98. Alekseev E I et al. *Radiotekh. Elektron.* **41** 759 (1996)
99. Alekseev E I et al. *Radiotekh. Elektron.* **41** 762 (1996)
100. Gelikonov V M et al. *Pis'ma Zh. Eksp. Teor. Fiz.* **61** 149 (1995) [*JETP Lett.* **61** 158 (1995)]
101. Jones R C *J. Opt. Soc. Am.* **31** 488 (1941)
102. Hurwitz H, Jones R C *J. Opt. Soc. Am.* **31** 493 (1941)
103. Jones R C *J. Opt. Soc. Am.* **31** 500 (1941)
104. Alekseev E I, Bazarov E N, Izraelyan V G *Kvantovaya Elektron.* **11** 397 (1984) [*Sov. J. Quantum Electron.* **14** 271 (1984)]
105. Shurkliff W A *Polarized Light* (Cambridge, Mass.: Harvard Univ. Press, 1962) [Translated into Russian (Moscow: Mir, 1965)]
106. Gorshkov M M *Ellipsometriya* (Ellipsometry) (Moscow: Sov. Radio, 1974)
107. Azzam R M A, Bashara N M *Ellipsometry and Polarized Light* (Amsterdam: North-Holland, 1977) [Translated into Russian (Moscow: Mir, 1981)]
108. Gerrard A, Burch J M *Introduction to Matrix Methods in Optics* (New York: Wiley, 1975) [Translated into Russian (Moscow: Mir, 1978)]
109. Yariv A, Yeh P *Optical Waves in Crystals: Propagation and Control of Laser Radiation* (New York: Wiley, 1984) [Translated into Russian (Moscow: Mir, 1987)]
110. Brosseau C *Fundamentals of Polarized Light: A Statistical Optics Approach* (New York: Wiley, 1998)
111. Gantmacher F R *Teoriya Matrits* (The Theory of Matrices) 2nd ed. (Moscow: Nauka, 1966) [Translation of the 1st Russian ed. (New York: Chelsea Publ. Co., 1959)]
112. Pavlath G A, Shaw H J *Appl. Opt.* **21** 1752 (1982)
113. Burns W K, Moeller R P *J. Lightwave Technol.* **LT-2** 430 (1984)
114. Kozel S M et al. *Opt. Spektrosk.* **61** 1295 (1986) [*Opt. Spectrosc.* **61** 814 (1986)]
115. Malykin G B *Izv. Vyssh. Uchebn. Zaved., Radiofiz.* **34** 817 (1991) [*Radiophys. Quantum Electron.* **34** 667 (1991)]
116. Malykin G B *Izv. Vyssh. Uchebn. Zaved., Radiofiz.* **35** 189 (1992) [*Radiophys. Quantum Electron.* **35** 134 (1992)]
117. Malykin G B *Opt. Spektrosk.* **75** 1314 (1993) [*Opt. Spectrosc.* **75** 775 (1993)]
118. Malykin G B *Opt. Spektrosk.* **83** 1013 (1997) [*Opt. Spectrosc.* **83** 937 (1997)]
119. Andronova I A, Gelikonov G V, Malykin G B *Kvantovaya Elektron.* **26** 271 (1999) [*Quantum Electron.* **29** 271 (1999)]
120. Andronova I A, Gelikonov G V, Malykin G B *Proc. SPIE* **3736** 423 (1999)
121. Ginzburg V L *Rasprostranenie Elektromagnitnykh Voln v Plazme* (Propagation of Electromagnetic Waves in Plasma) (Moscow: GIFML, 1960) [Translated into English (New York: Gordon and Breach, 1962) (Oxford: Pergamon Press, 1970)]
122. Landau L D, Lifshitz E M, Pitaevskiĭ L P *Elektrodinamika Sploshnykh Sred* (Electrodynamics of Continuous Media) (Moscow: Nauka, 1982) [Translated into English (Oxford: Pergamon Press, 1984)]
123. Novikov M A *Kristallografiya* **24** 666 (1979)
124. Andronova I A, Gelikonov V M, Gelikonov G V *Izv. Vyssh. Uchebn. Zaved., Radiofiz.* **41** 1448 (1998)
125. Malykin G B, Pozdnyakova V I *Opt. Spektrosk.* **84** 145 (1998) [*Opt. Spectrosc.* **84** 145 (1998)]
126. Malykin G B, Pozdnyakova V I *Opt. Spektrosk.* **86** 505 (1999) [*Opt. Spectrosc.* **86** 444 (1999)]
127. Malykin G B, Pozdnyakova V I *Opt. Spektrosk.* **86** 513 (1999) [*Opt. Spectrosc.* **86** 451 (1999)]
128. Malykin G B, Pozdnyakova V I *Opt. Spektrosk.* **89** 76 (2000) [*Opt. Spectrosc.* **89** 68 (2000)]
129. Schiffner G et al. *Appl. Opt.* **18** 2096 (1979)
130. Ulrich R, Johnson M *Opt. Lett.* **4** 152 (1979)
131. Logozinskiĭ V N "Issledovanie steklovolokonnogo interferometra kak datchika uglovoĭ skorosti" ("Investigation of a glass fiber interferometer as an angular velocity sensor"), Graduation Thesis (Moscow: Moscow Institute of Physics and Technology, 1979)
132. Gordon S A, Logozinskiĭ V N, Novikov A G *Kvantovaya Elektron.* **7** 2252 (1980) [*Sov. J. Quantum Electron.* **10** 1312 (1980)]
133. Gur'yanov A N et al. *Pis'ma Zh. Eksp. Teor. Fiz.* **32** 240 (1980) [*JETP Lett.* **32** 221 (1980)]
134. Kintner E C *Opt. Lett.* **6** 154 (1981)
135. Frins E M, Dultz W *Opt. Commun.* **136** 354 (1997)
136. Senthilkumaran P, Thursby G, Culshaw B *Opt. Lett.* **25** 533 (2000)
137. Senthilkumaran P, Culshaw B, Thursby G *J. Opt. Soc. Am. B* **17** 1914 (2000)
138. Rytov S M *Dokl. Akad. Nauk SSSR* **18** 263 (1938)
139. Rytov S M *Tr. Fiz. Inst. Akad. Nauk SSSR* **2** (1) 41 (1940)
140. VladimirskiĭV V *Dokl. Akad. Nauk SSSR* **31** 222 (1941)
141. Kravtsov Yu A, Orlov Yu I *Geometricheskaya Optika Neodnorodnykh Sred* (Geometrical Optics of Inhomogeneous Media) (Moscow: Nauka, 1980) [Translated into English (Berlin: Springer-Verlag, 1990)]
142. Berry M V *Proc. R. Soc. London Ser. A* **392** 45 (1984)
143. Berry M V *Nature* **326** 277 (1987)
144. Vinitskiĭ S I et al. *Usp. Fiz. Nauk* **160** (6) 1 (1990) [*Sov. Phys. Usp.* **33** 403 (1990)]
145. Berry M *Phys. Today* **43** (12) 34 (1990)
146. Anandan J *Nature* **360** 307 (1992)
147. Klyshko D N *Usp. Fiz. Nauk* **163** (11) 1 (1993) [*Phys. Usp.* **36** 1005 (1993)]
148. Bodnarchuk V I, Davtyan L S, Korneev D A *Usp. Fiz. Nauk* **166** 185 (1996) [*Phys. Usp.* **39** 169 (1996)]
149. Malykin G B *Izv. Vyssh. Uchebn. Zaved., Radiofiz.* **40** 265 (1997)
150. Itoh K, Saitoh T, Ohtsuka Y *J. Lightwave Technol.* **LT-5** 916 (1987)
151. Andronova I A, Gelikonov V M, Gelikonov G V *Kvantovaya Elektron.* **30** 115 (2000) [*Quantum Electron.* **30** 115 (2000)]
152. Varnham M P et al. *Opt. Lett.* **9** 306 (1984)
153. Okamoto K, Hosaka T, Noda J *J. Lightwave Technol.* **LT-3** 758 (1985)
154. Donati S et al. *IEEE Photonics Tech. Lett.* **7** 1174 (1995)
155. Moeller R P, Burns W K, Frigo N J *J. Lightwave Technol.* **7** 262 (1989)
156. Eickhoff W *Electron. Lett.* **16** 762 (1980)
157. Tsao C Y H, Payne D N, Li L *Appl. Opt.* **28** 588 (1989)
158. Wang A et al. *Opt. Lett.* **20** 279 (1995)
159. Bergh R A, Lefevre H C, Shaw H J *Opt. Lett.* **5** 479 (1980)
160. Liu K, Sorin W V, Shaw H J *Opt. Lett.* **11** 180 (1986)
161. Logozinski V, Glavatskih N, in *Symp. Gyro Technology 1992, Stuttgart, Germany, 22–23 September 1992* (Ed. H Sorg) (Stuttgart: Univ. Stuttgart, Inst. A. für Mechanik, Deutsche Gesellschaft für Ortung und Navigation, 1992) p. 40
162. Wakaki M et al. *Appl. Opt.* **35** 2591 (1996)
163. Birman A *Proc. SPIE* **2837** 368 (1996)
164. Varnham M P, Payne D N, Love J D *Electron. Lett.* **20** 55 (1984)
165. Vassallo C *J. Lightwave Technol.* **LT-5** 24 (1987)
166. Sader J E, Wong D *IEEE J. Quantum Electron.* **QE-28** 1533 (1992)
167. Kozel S M et al. *Opt. Spektrosk.* **59** 180 (1985) [*Opt. Spectrosc.* **59** 106 (1985)]
168. Listvin A V *Pis'ma Zh. Tekh. Fiz.* **20** (24) 19 (1994) [*Tech. Phys. Lett.* **20** 981 (1994)]
169. Izraelyan V G "Teoriya Volokonno-Opticheskikh Kol'tsevykh Interferometrov" ("Theory of Fiber-Optic Ring Interferometers"), Thesis for Candidate of Physicomathematical Sciences (Moscow: Institute of Radioengineering and Electronics, USSR Academy of Sciences, 1987)
170. Rashleigh S C, Ulrich R *Opt. Lett.* **3** 60 (1978)
171. Ulrich R, Simon A *Appl. Opt.* **18** 2241 (1979)
172. Barlow A J, Ramskov-Hansen J J, Payne D N *Appl. Opt.* **20** 2962 (1981)
173. Zheleznyakov V V, Kocharovskiĭ V V, Kocharovskiĭ Vl V *Usp. Fiz. Nauk* **141** 257 (1983) [*Sov. Phys. Usp.* **26** 877 (1983)]
174. Malykin G B, Pozdnyakova V I, Shereshevskiĭ I A *Opt. Spektrosk.* **83** 843 (1997) [*Opt. Spectrosc.* **83** 780 (1997)]
175. Malykin G B *Opt. Spektrosk.* **81** 474 (1996) [*Opt. Spectrosc.* **81** 431 (1996)]
176. Malykin G B *Opt. Spektrosk.* **84** 515 (1998) [*Opt. Spectrosc.* **84** 455 (1998)]
177. Böhm K, Petermann K, Weidel E *J. Lightwave Technol.* **LT-1** 71 (1983)

178. Fridricks R J, Ulrich R *Electron. Lett.* **20** 330 (1984)
179. Jones E, Parker J W *Electron. Lett.* **22** 54 (1986)
180. Tai S et al. *Electron. Lett.* **22** 546 (1986)
181. Listvin V N, Logozinskiĭ V N *Izv. Vyssh. Uchebn. Zaved., Radiofiz.* **34** 1001 (1991) [*Radiophys. Quantum Electron.* **34** 791 (1991)]
182. Alekseev E I, Bazarov E N *Kvantovaya Elektron.* **19** 897 (1992) [*Sov. J. Quantum Electron.* **22** 834 (1992)]
183. Malykin G B et al. *Izv. Vyssh. Uchebn. Zaved., Radiofiz.* **37** 1567 (1994)
184. Malykin G B, Pozdnyakova V I, Pozdnyakov E L *Izv. Vyssh. Uchebn. Zaved., Radiofiz.* **38** 1293 (1995) [*Radiophys. Quantum Electron.* **38** 845 (1995)]
185. Burns W K, Kersey A D *J. Lightwave Technol.* **10** 992 (1992)
186. Blake J, Szafraniec B, Feth J *Opt. Lett.* **21** 1192 (1996)
187. Szafraniec B, Sanders G A *J. Lightwave Technol.* **17** 579 (1999)
188. Ruffin P B, Baeder J, Sung C C *Opt. Eng.* **40** 605 (2001)
189. Lyot B *Ann. l'Observ. d'Astron. Paris* (Meudon) **8** 102 (1928)
190. Loeber A P *J. Opt. Soc. Am.* **72** 650 (1982)
191. Mochizuki K *Appl. Opt.* **23** 3284 (1984)
192. Cooper P R *Opt. Laser Technol.* **18** 99 (1986)
193. Wang J S, Costelloe J R, Stolen R H *IEEE Photonics Tech.* **11** 1449 (1999)
194. Dakin J, Culshaw B (Eds) *Optical Fiber Sensors* Vol. 1 *Principles and Components* (Boston: Artech House, 1988) [Translated into Russian (Moscow: Mir, 1992)]
195. Moeller R P, Burns W K *Electron. Lett.* **19** 187 (1983)
196. Zalogin A N, Kozel S M, Listvin V N *Izv. Vyssh. Uchebn. Zaved., Radiofiz.* **29** 243 (1986)
197. Malykin G B *Izv. Vyssh. Uchebn. Zaved., Radiofiz.* **35** 993 (1992) [*Radiophys. Quantum Electron.* **35** 637 (1992)]
198. Malykin G B, Nefedov I M, Shereshevskiĭ I A *Izv. Vyssh. Uchebn. Zaved., Radiofiz.* **37** 1473 (1994) [*Radiophys. Quantum Electron.* **37** 847 (1994)]
199. Alekseev E I, Bazarov E N *Radiotekhnika Elektron.* **42** 1148 (1997)
200. Lefevre H C *Electron. Lett.* **16** 778 (1980)
201. Takada K, Okamoto K, Noda J *J. Lightwave Technol.* **LT-4** 213 (1986)
202. Shen P, Palais J C, Lin C *Appl. Opt.* **37** 443 (1998)
203. Shen P, Palais J C *Appl. Opt.* **38** 1686 (1999)
204. Listvin A V, Listvin V N *Pis'ma Zh. Tekh. Fiz.* **21** (21) 29 (1995) [*Tech. Phys. Lett.* **21** 875 (1995)]
205. Alekseev E I et al. *Pis'ma Zh. Tekh. Fiz.* **9** 837 (1983)
206. Alekseev E I, Bazarov E N, Kurbatov A M *Pis'ma Zh. Tekh. Fiz.* **9** 885 (1983) [*Sov. Tech. Phys. Lett.* **9** 381 (1983)]
207. Alekseev E I et al. *Zh. Tekh. Fiz.* **55** 1648 (1985) [*Sov. Phys. Tech. Phys.* **30** 959 (1985)]
208. Billings B H *J. Opt. Soc. Am.* **41** 966 (1951)
209. Chien P-Y, Pan C-L *Opt. Lett.* **16** 189 (1991)
210. Marcuse D *Theory of Dielectric Optical Waveguides* (New York: Academic Press, 1974)
211. Marcuse D *Bell System Tech. J.* **54** 985 (1975)
212. Kaminow I P *IEEE J. Quantum Electron.* **QE-17** 15 (1981)
213. Rashleigh S C *J. Lightwave Technol.* **LT-1** 312 (1983)
214. Cancellieri G, Fantini P, Tilio M *J. Opt. Soc. Am. A* **2** 1885 (1985)
215. Takada K et al. *J. Opt. Soc. Am. A* **3** 1594 (1986)
216. Payne F P, Payne D N, Varnham M P *Res. J. Depart. Electron. Comp. Sci. Univ. Southampton* (Ed. A Pickering) 144 (1987)
217. Listvin A V, Listvin V N *Izv. Vyssh. Uchebn. Zaved., Radiofiz.* **38** 804 (1995) [*Radiophys. Quantum Electron.* **38** 531 (1995)]
218. Aleksandrov A Yu et al. *Radiotekhnika* (8) 90 (1988)
219. Marrone M J et al. *Opt. Lett.* **12** 60 (1987)
220. Kocharovskiĭ V V et al. *Izv. Ross. Akad. Nauk, Ser. Fiz.* **62** 362 (1998)
221. Malykin G B, Pozdnyakova V I, Shereshevskiĭ I A *Opt. Spektrosk.* **88** 477 (2000) [*Opt. Spectrosc.* **88** 427 (2000)]
222. Krawarik P H, Watkins L S *Appl. Opt.* **17** 3984 (1978)
223. Malykin G B *Opt. Spektrosk.* **91** 676 (2001) [*Opt. Spectrosc.* **91** 638 (2001)]
224. Ranka J K, Windeler R S, Stentz A J *Opt. Lett.* **25** 25 (2000)
225. Malykin G B, Pozdnyakova V I *Opt. Spektrosk.* **89** 299 (2000) [*Opt. Spectrosc.* **89** 273 (2000)]
226. Malykin G B, Pozdnyakova V I, Shereshevskiĭ I A *Izv. Vyssh. Uchebn. Zaved., Radiofiz.* **43** 976 (2000) [*Radiophys. Quantum Electron.* **43** 879 (2000)]
227. Malykin G B, Pozdnyakova V I, Shereshevskiĭ I A *Izv. Vyssh. Uchebn. Zaved., Radiofiz.* **43** 1078 (2000) [*Radiophys. Quantum Electron.* **43** 969 (2000)]
228. Malykin G B, Pozdnyakova V I, Shereshevskiĭ I A *Pis'ma Zh. Tekh. Fiz.* **27** (7) 40 (2001) [*Tech. Phys. Lett.* **27** 281 (2001)]
229. Malykin G B, Pozdnyakova V I, Shereshevskii I A *J. Opt. B: Quantum Semiclass. Opt.* **3** S93 (2001)
230. Ulrich R, Rashleigh S C *IEEE J. Quantum Electron.* **QE-18** 2032 (1982)
231. Malykin G B *Izv. Vyssh. Uchebn. Zaved., Radiofiz.* **37** 265 (1994) [*Radiophys. Quantum Electron.* **37** 159 (1994)]
232. Malykin G B *Izv. Vyssh. Uchebn. Zaved., Radiofiz.* **38** 604 (1995) [*Radiophys. Quantum Electron.* **38** 401 (1995)]
233. Bazarov E N et al. *Radiotekhnika Elektron.* **27** 2245 (1982)
234. Malykin G B *Pis'ma Zh. Tekh. Fiz.* **25** (16) 78 (1999) [*Tech. Phys. Lett.* **25** 668 (1999)]
235. Malykin G B, Nefedov I M, Shereshevskiĭ I A *Izv. Vyssh. Uchebn. Zaved., Radiofiz.* **37** 1473 (1994) [*Radiophys. Quantum Electron.* **37** 847 (1994)]
236. Andronova I A et al. *Izv. Vyssh. Uchebn. Zaved., Radiofiz.* **40** 780 (1997)
237. Fadeev A V *Izv. Vyssh. Uchebn. Zaved., Priborostr.* **33** (8) 69 (1990)
238. Mortimore D B *J. Lightwave Technol.* **6** 1217 (1988)
239. Birks T A, Morkel P R *Appl. Opt.* **27** 3107 (1988)
240. Shupe D M *Appl. Opt.* **19** 654 (1980)
241. Bazarov E N et al. *Opt. Spektrosk.* **55** 190 (1983)
242. Bergh R A, Lefevre H C, Shaw H J *Opt. Lett.* **6** 502 (1981)
243. Andronova I A et al. *Izv. Vyssh. Uchebn. Zaved., Radiofiz.* **34** 412 (1991) [*Radiophys. Quantum Electron.* **34** 346 (1991)]
244. Andreev A Ts et al. *Zh. Tekh. Fiz.* **63** (12) 62 (1993) [*Tech. Phys.* **38** 1067 (1993)]
245. Alekseev E I et al. *Radiotekhnika Elektron.* **42** 1150 (1997)
246. Gangding P, Shangyuan H, Zongqi L *Electron. Lett.* **22** 1337 (1989)
247. Andronova I A, Gelikonov V M, Stepanov D P *Kvantovaya Elektron.* **21** 863 (1994) [*Quantum Electron.* **24** 805 (1994)]
248. Szafraniec B, Blake J *J. Lightwave Technol.* **12** 1679 (1994)
249. Jeong H J et al. *Opt. Lett.* **19** 1421 (1994)
250. Gelikonov V M et al. *Pis'ma Zh. Tekh. Fiz.* **13** 775 (1987)
251. Gelikonov V M, Leonov V I, Novikov M A *Kvantovaya Elektron.* **16** 1905 (1989) [*Sov. J. Quantum Electron.* **19** 1227 (1989)]
252. Martinelli M *Opt. Commun.* **72** 341 (1989)
253. Alekseev E I, Bazarov E N *Pis'ma Zh. Tekh. Fiz.* **23** (15) 90 (1997) [*Tech. Phys. Lett.* **23** 613 (1997)]
254. Alekseev E I et al. *Radiotekhnika Elektron.* **44** 122 (1999)
255. Welker D J et al. *Opt. Lett.* **23** 1826 (1998)
256. Jackson S M et al. *J. Lightwave Technol.* **16** 2016 (1998)
257. Ner M S, Kemmler M W, Spahlinger G *Proc. SPIE* **2837** 335 (1996)
258. Kim B Y et al. *Proc. SPIE* **425** 86 (1983)
259. Malykin G B *Izv. Vyssh. Uchebn. Zaved., Radiofiz.* **37** 1345 (1994)
260. Malykin G B *Izv. Vyssh. Uchebn. Zaved., Radiofiz.* **39** 624 (1996)
261. Böhm K, Petermann K, Weidel E *Opt. Lett.* **7** 180 (1982)
262. Böhm K, Petermann K, Weidel E, in *Fiber-Optic Rotation Sensors and Related Technologies: Proc. of the 1st Intern. Conf., MIT, Cambridge, Mass., USA, November 9–11, 1981* (Springer Ser. in Optical Sciences, Vol. 32, Eds S Ezekiel, H J Arditty) (Berlin: Springer-Verlag, 1982) p. 337
263. Hotate K, Tabe K *Appl. Opt.* **25** 1086 (1986)
264. Tabe K, Hotate K *Opt. Acta* **33** 1553 (1986)
265. Galkin S L, Kozhevnikov R M *Opt. Spektrosk.* **62** 170 (1987) [*Opt. Spectrosc.* **62** 103 (1987)]
266. Hotate K, Tabe K *J. Lightwave Technol.* **LT-5** 997 (1987)
267. Saida T, Hotate K *J. Lightwave Technol.* **17** 222 (1999)
268. Blake J *Proc. SPIE* **1367** 81 (1991)
269. Stolen R H, Ashkin A *Appl. Phys. Lett.* **22** 294 (1973)
270. Birman A Ya, Logozinskiĭ V N *Kvantovaya Elektron.* **9** 410 (1982) [*Sov. J. Quantum Electron.* **12** 236 (1982)]
271. Bergh R A, Lefevre H C, Shaw H J *Opt. Lett.* **7** 282 (1982)
272. Ezekiel S, Davis J L, Hellwarth R W *Opt. Lett.* **7** 457 (1982)
273. Ezekiel S, Davis J L, Hellwarth R W, in *Fiber-Optic Rotation Sensors and Related Technologies: Proc. of the 1st Intern. Conf., MIT, Cambridge, Mass., USA, November 9–11, 1981* (Springer Ser. in Optical Sciences, Vol. 32, Eds S Ezekiel, H J Arditty) (Berlin: Springer-Verlag, 1982) p. 332

274. Milovskiĭ N D, Sheshin V Yu *Zh. Eksp. Teor. Fiz.* **107** 1826 (1995) [*JETP* **80** 1013 (1995)]
275. Milovskiĭ N D *Izv. Vyssh. Uchebn. Zaved., Radiofiz.* **38** 318 (1995)
276. Milovskiĭ N D, Fedyaev O E *Opt. Spektrosk.* **82** 615 (1997) [*Opt. Spectrosc.* **82** 568 (1997)]
277. Gelikonov V M et al. *Izv. Vyssh. Uchebn. Zaved., Radiofiz.* **42** 1054 (1999) [*Radiophys. Quantum Electron.* **42** 928 (1999)]
278. Bergh R A et al. *Opt. Lett.* **7** 563 (1982)
279. Frigo N J et al. *Opt. Lett.* **8** 119 (1983)
280. Crosignani B, Yariv A *J. Lightwave Technol.* **LT-3** 914 (1985)
281. Malykin G B *Opt. Spektrosk.* **91** 846 (2001) [*Opt. Spectrosc.* **91** 795 (2001)]
282. Zakhidov E A et al. *Kvantovaya Elektron.* **15** 2525 (1988) [*Sov. J. Quantum Electron.* **18** 1586 (1988)]
283. Lamouroux B F, Prade B S, Vinet J-Y *Appl. Opt.* **29** 750 (1990)
284. Wieman C, Hänsch T W *Phys. Rev. Lett.* **36** 1170 (1976)
285. Sargent III M *Phys. Rev. A* **14** 524 (1976)
286. Yakubovich E I *Zh. Eksp. Teor. Fiz.* **56** 676 (1969) [*Sov. Phys. JETP* **29** 368 (1969)]
287. Crosignani B, Daino B, Di Porto P *J. Opt. Soc. Am. B* **3** 1120 (1986)
288. Zborovskiĭ V A, Fradkin E E *Zh. Eksp. Teor. Fiz.* **66** 1217 (1974) [*Sov. Phys. JETP* **39** 595 (1974)]
289. Zborovskiĭ V A, Tiunov E A, Fradkin E E *Izv. Vyssh. Uchebn. Zaved., Radiofiz.* **21** 816 (1978) [*Radiophys. Quantum Electron.* **21** 576 (1978)]
290. Birman A Ya, Savushkin A F *Opt. Spektrosk.* **39** 135 (1975) [*Opt. Spectrosc.* **39** 77 (1975)]
291. Fateev V F *Opt. Spektrosk.* **50** 30 (1981) [*Opt. Spectrosc.* **50** 14 (1981)]
292. Fateev V F *Radiotekhnika Elektron.* **28** 164 (1983)
293. Lense J, Thirring H *Phys. Z.* **19** 156 (1918)
294. Silberstein L T *J. Opt. Soc. Am.* **5** 291 (1921)
295. Scully M O, Zubairy M S, Haugan M P *Phys. Rev. A* **24** 2009 (1981)
296. Tartaglia A *Phys. Rev. D* **58** 064009 (1998)
297. Kingsley S A, in *Fiber-Optic Rotation Sensors and Related Technologies: Proc. of the 1st Intern. Conf., MIT, Cambridge, Mass., USA, November 9 – 11, 1981* (Springer Ser. in Optical Sciences, Vol. 32, Eds S Ezekiel, H J Arditty) (Berlin: Springer-Verlag, 1982) p. 386
298. Beyersdorf P T, Fejer M M, Byer R L *Opt. Lett.* **24** 1112 (1999)
299. Beyersdorf P T, Fejer M M, Byer R L *J. Opt. Soc. Am. B* **16** 1354 (1999)
300. Sun K-X et al. *Phys. Rev. Lett.* **76** 3053 (1996)
301. Novikov M A *Radiotekhnika Elektron.* **21** 903 (1976)
302. Novikov M A *Opt. Spektrosk.* **61** 424 (1986) [*Opt. Spectrosc.* **61** 266 (1986)]
303. Thomas L H *Nature* **117** 514 (1926)
304. Thomas L H *Philos. Mag.* **3** 1 (1927)
305. Malykin G B, Permitin G V, in *Fizicheskaya Entsiklopediya* (Encyclopedia of Physics) (Ed. A M Prokhorov) Vol. 5 (Moscow: Bol'shaya Ross. Éntsiklopediya, 1998) p. 123
306. Malykin G B *Usp. Fiz. Nauk* **169** 585 (1999) [*Phys. Usp.* **42** 505 (1999)]
307. Malykin G B *Prikl. Matem. Mekh.* **63** 775 (1999)
308. Malykin G B *Izv. Ross. Akad. Nauk, Ser. Mekh. Tverd. Tela* (4) 187 (2000)
309. Anandan J *Phys. Rev. D* **24** 338 (1981)
310. Mashhoon B *Phys. Rev. Lett.* **61** 2639 (1988)
311. Berestetskiĭ V B, Lifshitz E M, Pitaevskiĭ L P *Kvantovaya Elektrodinamika* (Quantum Electrodynamics) (Moscow: Nauka, 1989) p. 41 [Translated into English (Oxford: Pergamon Press, 1982)]
312. Wagner J W, Spicer J B *J. Opt. Soc. Am. B* **4** 1316 (1987)
313. Logozinskiĭ V N *Kvantovaya Elektron.* **8** 895 (1981) [*Sov. J. Quantum Electron.* **11** 536 (1981)]
314. Logozinskiĭ V N, Novikov A G *Kvantovaya Elektron.* **9** 775 (1982) [*Sov. J. Quantum Electron.* **12** 479 (1982)]
315. Polukhin A T, Telegin G I *Kvantovaya Elektron.* **11** 387 (1984) [*Sov. J. Quantum Electron.* **14** 263 (1984)]
316. Alekseev E I *Kvantovaya Elektron.* **14** 192 (1987) [*Sov. J. Quantum Electron.* **17** 112 (1987)]
317. Peng G-D, Huang S-Y, Lin Z-Q *Opt. Lett.* **12** 434 (1987)
318. Andronova I A et al. *Zh. Tekh. Fiz.* **60** 216 (1990)
319. Burns W K, Moeller R P, Dandridge A *IEEE Photonics Tech. Lett.* **2** 606 (1990)
320. Moeller R P, Burns W K *Opt. Lett.* **16** 1902 (1991)
321. Blake J, Kim I S *Opt. Lett.* **19** 1648 (1994)
322. Belanov A S, Polukhin A T *Opt. Spektrosk.* **78** 281 (1995) [*Opt. Spectrosc.* **78** 251 (1995)]
323. Knudsen S, Blötekjaer K *Opt. Lett.* **20** 1432 (1995)
324. Moeller R P, Burns W K *Opt. Lett.* **21** 171 (1996)
325. Burns W K, Moeller R P *Proc. SPIE* **2837** 381 (1996)
326. Mohr F *J. Lightwave Technol.* **14** 27 (1996)
327. Wanser K H *Electron. Lett.* **28** 53 (1992)
328. Shabanov D V *Izv. Vyssh. Uchebn. Zaved., Radiofiz.* **43** 350 (2000) [*Radiophys. Quantum Electron.* **43** 317 (2000)]
329. Rabelo R C, de Carvalho R T, Blake J *J. Lightwave Technol.* **18** 2146 (2000)
330. Böhm K, Petermann K *Proc. SPIE* **719** 36 (1986)
331. Böhm K, Marten P, Weidel E *Electron. Lett.* **19** 997 (1983)
332. Eberhard D, Voges E *Opt. Lett.* **9** 22 (1984)
333. Kim B Y, Shaw H J *Opt. Lett.* **9** 378 (1984)
334. Kim B Y, Shaw H J *Opt. Lett.* **9** 375 (1984)
335. Ebberg A, Schiffner G *Opt. Lett.* **10** 300 (1985)
336. Kiesel E *Proc. SPIE* **838** 129 (1987)
337. Kim B Y et al. *IEE Conf. Publ.* **221** 136 (1983)
338. Udd E, Michal R J, Cahill R F *Proc. SPIE* **478** 136 (1984)
339. Frigo N J *Proc. SPIE* **719** 155 (1986)
340. Kersey A D, Dandridge A, Burns W K *Electron. Lett.* **22** 935 (1986)
341. Lefevre H C et al., in *Proc. 3rd Intern. Conf. on Optical Fiber Sensors (OFS'85), 1985*, Technical Digest, Ser. PDS 7.1
342. Kay C J *IEE Proc. J. Optoelectron.* **132** 259 (1985)
343. Hotate K et al. *Opt. Lett.* **7** 331 (1982)
344. Toyama K et al. *Opt. Lett.* **16** 1207 (1991)
345. Gronau Y, Tur M *Appl. Opt.* **34** 5849 (1995)
346. Chien P-Y, Chang Y-S, Chang M-W *Opt. Commun.* **135** 198 (1997)
347. Donati S, Annovazzi-Lodi V, in *Fiber-Optic Rotation Sensors and Related Technologies: Proc. of the 1st Intern. Conf., MIT, Cambridge, Mass., USA, November 9 – 11, 1981* (Springer Ser. in Optical Sciences, Vol. 32, Eds S Ezekiel, H J Arditty) (Berlin: Springer-Verlag, 1982) p. 292
348. Jackson D A, Kersey A D, Lewin A C *Electron. Lett.* **20** 399 (1984)
349. Culshaw B, Giles J P *IEEE J. Quantum Electron.* **QE-18** 690 (1982)
350. Kersey A D, Lewin A C, Jackson D A *Electron. Lett.* **20** 368 (1984)
351. Peng G-D, Huang S-Y, Lin Z-Q *J. Lightwave Technol.* **LT-5** 986 (1987)
352. Bukhman A B et al. *Pis'ma Zh. Tekh. Fiz.* **8** 897 (1982)
353. Udd E *Proc. SPIE* **425** 90 (1983)
354. Graingorge P, Arditty H "Hydrophone a fibre optique", French Patent N 2541767 (Aug. 31, 1984, filed Febr. 25, 1983)
355. Kråkenes K, Blötekjaer K *Opt. Lett.* **14** 1152 (1989)
356. Tanaka T et al. *Appl. Opt.* **33** 120 (1994)
357. Dyott R B *Electron. Lett.* **30** 1087 (1994)
358. Pavlath G A *Proc. SPIE* **2837** 46 (1996)
359. Sanders G A et al. *Proc. SPIE* **2837** 61 (1996)
360. Sakuma K *Proc. SPIE* **2837** 72 (1996)
361. Burns W K *Opt. Photonics News* **9** (5) 28 (1998)
362. Tselikov A, Blake J *Appl. Opt.* **37** 6690 (1998)
363. Malykin G B *Opt. Spektrosk.* **80** 280 (1996) [*Opt. Spectrosc.* **80** 245 (1996)]
364. Andronova I A, Mamaev Yu A *Opt. Spektrosk.* **80** 108 (1996) [*Opt. Spectrosc.* **80** 95 (1996)]
365. Chow W W et al. *Rev. Mod. Phys.* **57** 61 (1985)
366. de Carvalho R T, Blake J N *Proc. SPIE* **2837** 183 (1996)
367. Belov A V et al. *Kvantovaya Elektron.* **15** 2152 (1988) [*Sov. J. Quantum Electron.* **18** 1351 (1988)]
368. Abedin K S, Hyodo M, Onodera N *Opt. Lett.* **25** 299 (2000)
369. Olsson B-E, Karlsson M, Andrekson P A *IEEE Photonics Tech. Lett.* **10** 997 (1998)
370. Artiglia M et al. *Opt. Fiber Technol.* **2** 75 (1996)
371. Shirai T, Barnes T H, Haskel T G *Opt. Lett.* **24** 297 (1999)
372. Carolan T A et al. *Appl. Opt.* **36** 380 (1997)
373. Blake J N *Proc. SPIE* **2837** 166 (1996)
374. Short S X et al. *J. Lightwave Technol.* **16** 1212 (1998)
375. Short S X et al. *J. Lightwave Technol.* **16** 1844 (1998)
376. Kang H S, Lee J H, Lee K S *IEEE Photonics Tech. Lett.* **10** 1464 (1998)
377. Lin H, Lin W-W, Chen M-H *Appl. Opt.* **38** 2760 (1999)

378. Rose A H, Etzel S M, Rochford K B *J. Lightwave Technol.* **17** 1042 (1999)
379. Bergh R A, Lefevre H C, Shaw H J, in *Fiber-Optic Rotation Sensors and Related Technologies: Proc. of the 1st Intern. Conf., MIT, Cambridge, Mass., USA, November 9–11, 1981* (Springer Ser. in Optical Sciences, Vol. 32, Eds S Ezekiel, H J Arditty) (Berlin: Springer-Verlag, 1982) p. 405
380. Zheng G et al. *Proc. SPIE* **2837** 177 (1996)
381. Andreev A Ts et al. *Kvantovaya Elektron.* **20** 791 (1993) [*Quantum Electron.* **23** 685 (1993)]
382. Starodumov A N et al. *Appl. Phys. Lett.* **70** 19 (1997)
383. Tapia-Mercado J, Khomenko A V, Garcia-Weidner A *J. Lightwave Technol.* **19** 70 (2001)
384. Jinno M, Matsumoto T *IEEE J. Quantum Electron.* **QE-28** 875 (1992)
385. Wong W S et al. *Opt. Lett.* **22** 1150 (1997)
386. Shcherbakov A S, Koroleva Yu V *Opt. Spektrosk.* **83** 1045 (1997) [*Opt. Spectrosc.* **83** 964 (1997)]
387. Kuzin E A et al. *Opt. Commun.* **144** 60 (1997)
388. Rhy H Y, Kim B Y, Lee H-W *Opt. Commun.* **147** 47 (1998)
389. McBride R et al., in *Proc. of the 5th Intern. Symp. on Application of Laser Techniques to Fluid Mechanics, Lisbon, Portugal, 9–12 July, 1990*
390. Cooper D G, Dexter J L, Esman R D *IEEE J. Selected Topics Quantum Electron.* **1** 14 (1995)
391. Hong J B et al. *IEEE Photonics Tech. Lett.* **11** 1030 (1999)
392. Haus J W et al. *Opt. Lett.* **24** 376 (1999)
393. Serkland D K, Kumar P *Opt. Lett.* **24** 92 (1999)
394. Lim D S et al. *Opt. Lett.* **23** 1671 (1998)
395. Mendlovic D, Shabtay G, Lohmann A W *Opt. Lett.* **24** 361 (1999)
396. Butler D L et al. *Opt. Lett.* **20** 560 (1995)
397. Shcherbakov A A, Swart P L *J. Lightwave Technol.* **16** 1404 (1998)
398. Vakoc B J et al. *J. Lightwave Technol.* **17** 2316 (1999)
399. Kuzin E A, Núñez H C, Korneev N *Opt. Commun.* **160** 37 (1999)
400. Udd E *Proc. SPIE* **2837** 172 (1996)
401. Havstad S A et al. *Opt. Lett.* **24** 1466 (1999)
402. Madsen C K et al. *Opt. Lett.* **24** 1555 (1999)
403. Blake J et al. *Proc. SPIE* **1694** 188 (1992)
404. Liu R-Y et al. *Proc. SPIE* **2837** 82 (1996)
405. Ha J C et al. *Proc. SPIE* **2837** 152 (1996)
406. Ruffin P B et al. *Proc. SPIE* **2837** 345 (1996)
407. Kajioka H et al. *Proc. SPIE* **2837** 18 (1996)
408. *Selected Papers on Fiber-Optic Gyroscopes* (SPIE Milestone Ser., Vol. MS 8, Ed. R B Smith) (Bellingham, Wash.: SPIE Optical Eng. Press, 1989)
409. Yu A, Siddiqui A S *Electron. Lett.* **28** 1778 (1992)
410. Kringlebotn J T, Blötekjaer K, Pannell C N *Fiber Integrated Opt.* **14** 265 (1995)
411. Hu Z et al. *Proc. SPIE* **3860** 348 (1999)
412. Hotate K *Proc. SPIE* **2837** 33 (1996)
413. Ivanov V V, Novikov M A, Gelikonov V M *Pis'ma Zh. Tekh. Fiz.* **25** (23) 34 (1999) [*Tech. Phys. Lett.* **25** 940 (1999)]
414. Ivanov V V, Novikov M A, Gelikonov V M *Kvantovaya Elektron.* **30** 119 (2000) [*Quantum Electron.* **30** 119 (2000)]